EM-Neuro Modeling Across Scales for Bioelectronic Medicine

Lecture 6: Spinal cord stimulation for neuroprosthetics and pain management & low-frequency exposure safety

Esra Neufeld[*] and Taylor Newton[*†]

[*]IT'IS Foundation for Research on Information Technologies in Society

[†]Integrated Systems Laboratory, ETH Zurich

Outline for Today

- Introduction & Clinical Motivation
- SCS Fundamentals - Dorsal Column vs. Root Targeting
- Lead Design, Placement & Optimization (incl. GAF)
- Clinical Results & Validation (STIMO Trial)
- Low-Frequency Exposure Safety Principles
- Simulation Tools & Coupled EM-Neuro Workflow

Course Outline

DATE	LECTURE THEME
19.02	Motivation, logistics & tooling (EN, TNE)
26.02	Ion channels & membranes (EN)
05.03	Axon models, activating functions & electrical stimulation (EN)
12.03	EM field simulation fundamentals & coupled EM-neuro workflows (EN)
19.03	Peripheral nerves & interfaces for bioelectronic medicine (EN)
26.03	Spinal cord stimulation for neuroprosthetics and pain management & low-frequency exposure safety (TNE)
02.04	Morphology, synapses, microcircuits; point vs spiking networks (TNE)
09.04	No class: Easter break
16.04	Neural mass & whole brain models; hybridization (TNE)
23.04	Recording modalities, signal content & the reciprocity theorem (TNE)
30.04	Non invasive brain stimulation & temporal interference (TNE)
07.05	Image based/personalized treatment planning and optimization (EN)
14.05	No class: Ascension Day
21.05	Verification, validation, UQ, and reproducibility (EN)
28.05	Project presentations & synthesis (EN, TNE)

Room: ETZ E7

13:15-14:00 Lecture

14:00-14:15 Break

14:15-15:00 Lecture

14:00-14:15 Break

15:15-16:00 Exercise

Recorded Lectures & Course Material

Provided Here

(CC BY License)

Exercise Outline

DATE	EXERCISE THEME
19.02	"Hello Neuron": integrate-and-fire in Python/NEURON
26.02	Point neuron phase portrait; basic time integration numerics
05.03	Recruitment prediction for myelinated axon using AF/GAF
12.03	EM (FEM) modeling of transcranial brain stimulation
19.03	Stimulation selectivity and signal content modeling for nerve interfaces
26.03	Guest (SCS – NeuroRestore)
02.04	Mini project work
09.04	No class: Easter break
16.04	Guest (Neuromodulation Spin-Off – Z43)
23.04	Mini project work
30.04	Guest (NIBS – Kinderspital)
07.05	Mini project work
14.05	No class: Ascension Day
21.05	Mini project work
28.05	Project presentations

Room: ETZ E7

13:15-14:00 Lecture

14:00-14:15 Break

14:15-15:00 Lecture

14:00-14:15 Break

15:15-16:00 Exercise

Learning Objectives

- Explain the historical trajectory from gate control theory [1] through Shealy's first dorsal column implant [2] to modern SCS paradigms
- Distinguish dorsal column versus dorsal root recruitment mechanisms and explain why this distinction matters for locomotor restoration versus pain relief [3], [4]
- Describe the STIMO/STIMO-2 patient-specific computational pipeline: MRI → segmentation → EM simulation → neuronal dynamics → recruitment optimization [5], [6]
- Apply activating function analysis [7] to predict which neural elements are excited by an epidural electrode configuration
- Connect lead placement, contact geometry, and pulse programming to predicted neural activation and selectivity [8], [9]
- Derive the rationale for low-frequency exposure safety limits from nerve stimulation biophysics [10], [11]
- Explain MRI safety principles including RF heating (SAR), gradient-induced PNS, and active implant considerations [12], [13]
- Articulate the unifying theme: the same cable-equation physics governs both therapeutic SCS optimization and electromagnetic safety assessment

Recommended Reading

- Wagner et al. (2018). Targeted neurotechnology restores walking in humans with spinal cord injury. Nature 563:65–71 [5]
- Rowald et al. (2022). Activity-dependent spinal cord neuromodulation rapidly restores trunk and leg motor functions after complete paralysis. Nat. Med. 28:260–271 [6]
- Capogrosso et al. (2013). A computational model for epidural electrical stimulation of spinal sensorimotor circuits. J. Neurosci. 33:19326–19340 [3]
- McIntyre et al. (2002). Modeling the excitability of mammalian nerve fibers. J. Neurophysiol. 87:995–1006 [14]
- Kapural et al. (2015). SENZA-RCT. Anesthesiology 123:851–860 [15]
- Reilly, J. Patrick, and Alan M. Diamant. *Electrostimulation: theory, applications, and computational model*. Artech House, 2011.

From: Wagner et al. (2018)

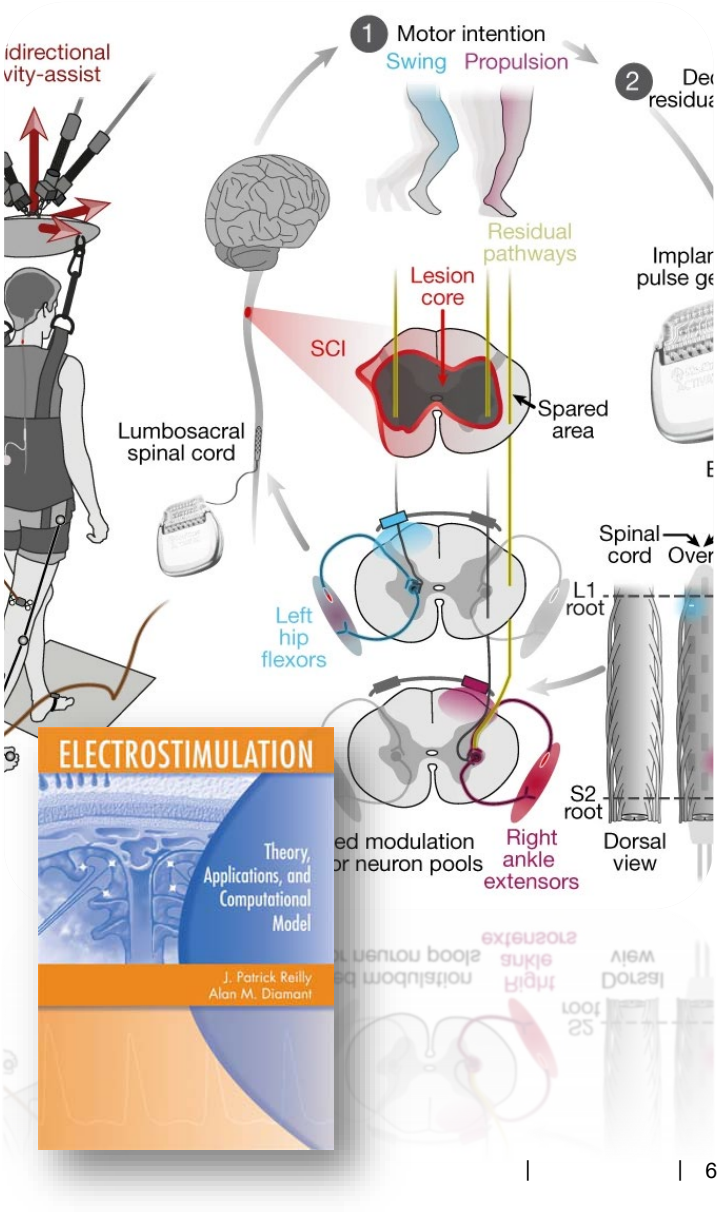

Spinal Cord Injury Epidemiology

- ~250,000–500,000 new spinal cord injuries per year worldwide [17]
- Age-standardized incidence declined from 13.0 to 9.5 per 100,000 (1990–2019), but prevalence increased due to improved survival [17]
- Devastating impact on quality of life, mobility, autonomy, and lifetime healthcare costs
- Standard of care offers limited motor recovery after the sub-acute rehabilitation phase
- Epidural electrical stimulation (EES) shows promise for chronic-phase patients — the focus of this lecture

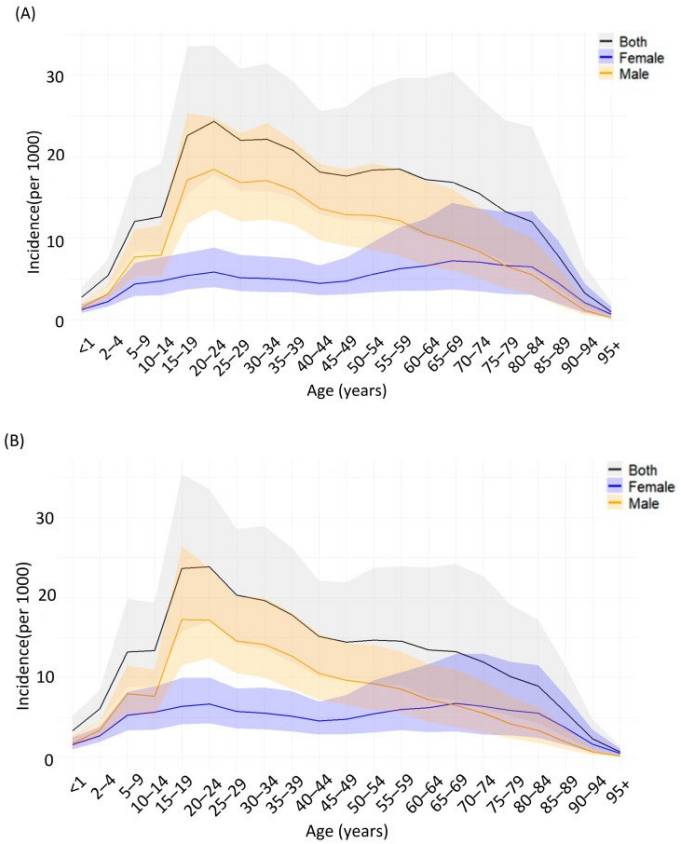

Age- and sex-specific incidence of spinal cord injuries globally in 2021. (**A**) Incidence of neck-level spinal cord injuries per 100,000 population by age group and sex. (**B**) Incidence of below-neck-level spinal cord injuries per 100,000 population by age group and sex. Image: [1].

From Acute Care to Chronic Plateau

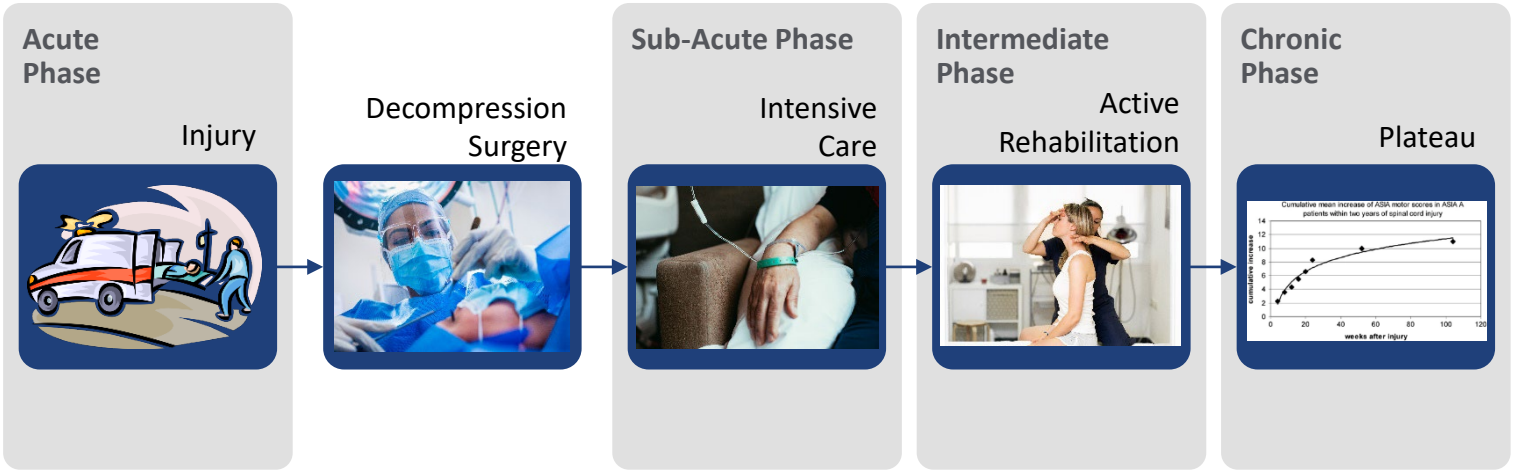

- **Acute phase** (hours): Decompression surgery within 24 h when indicated
- **Sub-acute phase** (~7 days): Intensive care and medical stabilization
- **Intermediate phase** (3–6 months): Active rehabilitation — most neurological recovery occurs here
- **Chronic phase** (12+ months): Functional plateau — historically, little or no further motor recovery (Image: [2])
- ***Key message*:** EES targets chronic-phase patients where conventional rehabilitation has reached its ceiling [5], [6]

Outline for Today

- **SCS History: Gate control to modern paradigms**
- Biophysics: Dorsal column vs. dorsal root recruitment
- STIMO Breakthrough: Clinical results & translation
- Personalized Pipeline: The STIMO-2 case study
- Exposure Safety: LF limits, MRI safety, implant considerations

Gate Control: Conceptual Foundation

- Melzack & Wall (Science, 1965): a neural “gate” in the substantia gelatinosa of the spinal dorsal horn modulates pain transmission [1]
- Large-diameter myelinated Aβ fibers → activate inhibitory interneurons → “close the gate” on nociceptive (small diameter) C- and Aδ-fiber signals
- Small-diameter nociceptive fibers → suppress inhibition → “open the gate”
- Also incorporated descending modulation from the brain — integrating cognitive and emotional factors into pain processing for the first time [18]
- Direct clinical implication: electrical stimulation of large-diameter fibers should produce analgesia
- Ended a century-long debate between specificity theory and pattern theory of pain

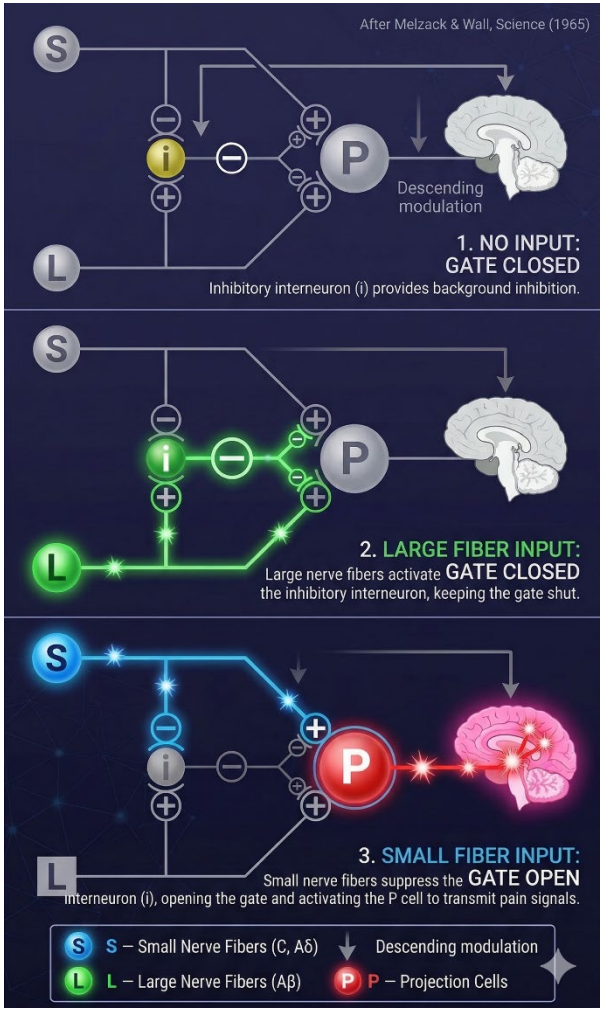

Image: [3]

From Theory to Therapy: Shealy's First Implant

- March 24, 1967: C. Norman Shealy performed the first dorsal column stimulation implant at Western Reserve University (now Case Western Reserve), Cleveland [2]
- Patient: bronchogenic carcinoma with intractable right lower chest pain
- Technique: bipolar intradural electrode placed via high-thoracic laminectomy (remove of vertebrae)
- Collaborators: J. Thomas Mortimer and James B. Reswick
- By 1968: Medtronic released the first commercially available SCS system [19]
- Subsequent reports (1970–1975): Shealy described outcomes in up to 80 patients, estimating ~75% efficacy for organic pain [19]
- Remarkably rapid bench-to-bedside translation: 2 years from Melzack & Wall's theory to first human implant

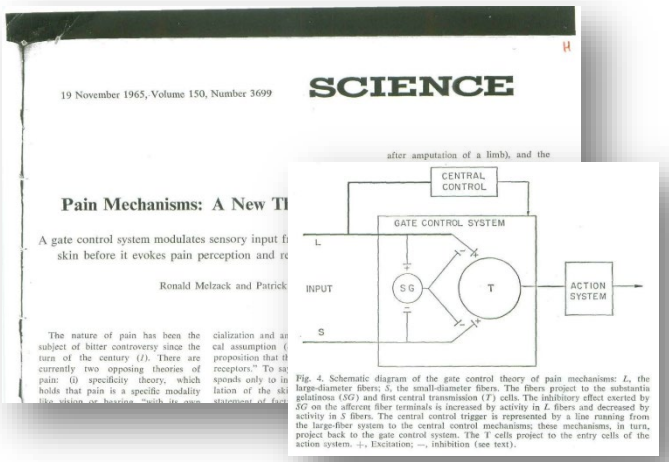

2 years…

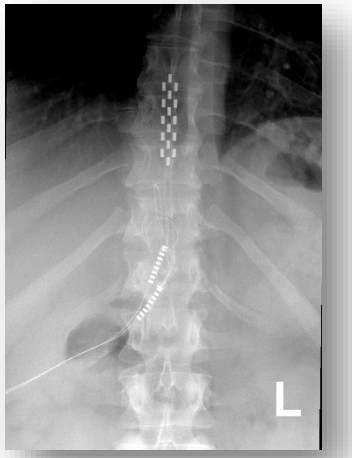

Image: [4]

Four Generations of Pain SCS

- **Tonic SCS** (1960s–present): 40–60 Hz continuous; paresthesia-based; dorsal column Aβ fibers [20]
- **Burst SCS** (De Ridder, 2010): 5 spikes at 500 Hz in 40-Hz packets; mimics thalamocortical firing [21]
  - SUNBURST trial: 100 subjects, 20 sites — burst superior to tonic ($p < 0.017$); 70.8% preferred burst [22]
  - FDA approval: Oct 2016 (Abbott BurstDR)
- **HF10 kHz SCS** (Nevro Senza, 2015): sub-perception, paresthesia-free [15]
  - SENZA-RCT: 84.5% vs. 43.8% back pain responder rate ($p < 0.001$) [15]
  - FDA PMA: May, 2015 — first-ever superiority labeling in SCS [23]
- **DRG stimulation** (St. Jude Medical Axium; later Abbott Proclaim DRG); targets dorsal root ganglion for focal pain [25]
  - ACCURATE trial: 152 patients — 81.2% vs. 55.7% success for CRPS ($p < 0.001$) [25]
  - FDA approval: Feb 2016

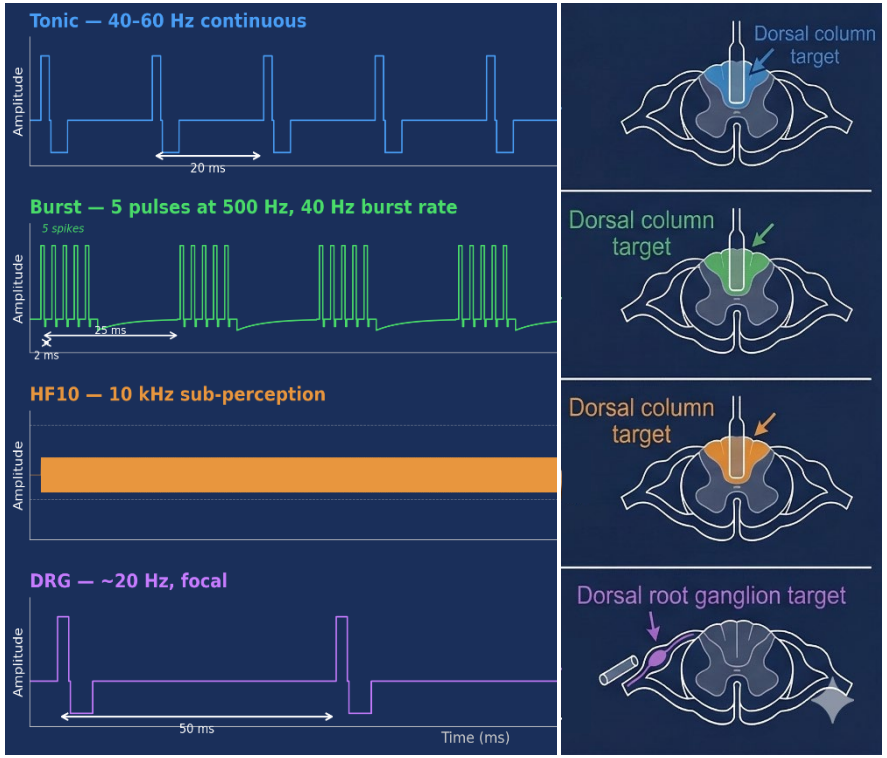

Image: [5]

Closed-Loop SCS

- **Open-loop limitation:** stimulation dose varies with posture, activity, and electrode migration; patients must manually re-program → suboptimal relief, overstimulation risk
- **Saluda Medical EVOKE trial** — first double-blind RCT in SCS history [26]
  - 134 patients randomized 1:1: ECAP-controlled closed-loop (CL) vs. fixed-output open-loop (OL)
  - ECAP = evoked compound action potential measured after every stimulation pulse
  - PID controller adjusts current >100×/second to maintain neural activation in therapeutic window

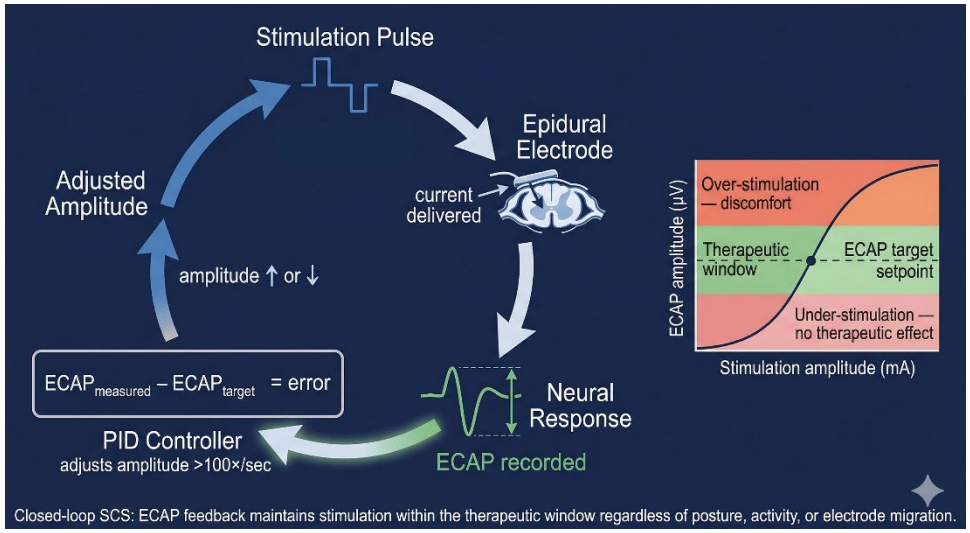

Closed-loop SCS: ECAP feedback maintains stimulation within the therapeutic window regardless of posture, activity, or electrode migration.

- **Results:** 83.1% CL vs. 61.0% OL achieved ≥50% pain reduction at 12 months [26]; 78% sustained at 36 months with zero explants for efficacy loss [27]
- **FDA approval:** Evoke system, Feb 2022
- **Medtronic Inceptiv:** first Medtronic ECAP-sensing closed-loop SCS platform; FDA approved 2024 [28]
- **Clinical lesson:** feedback control stabilizes the therapeutic window — a concept extending directly to locomotor SCS

Image: [6]

Spine Anatomy & Physiology: A Quick Primer

- **Dorsal roots:** sensory **afferents** entering the cord at each spinal level
  - fibers: Ia/Ib/II — proprioception; Aβ — touch, pressure, Aδ/C — pain, temperature
  - Ia afferents synapse onto α-motoneurons and spinal locomotor interneuron circuits
- **Dorsal columns: afferent** (ascending) white matter tracts carrying touch, vibration, and proprioceptive signals to brainstem
  - Relay information upward, but do not connect to spinal motor circuits
- **Ventral roots: efferent** motor axons (α- and γ-motoneurons) exiting the cord to innervate skeletal muscle
  - All voluntary and reflex movement passes through these
- **Ventral and lateral columns: mostly efferent** (descending) motor tracts carrying commands from the brain to spinal motoneurons and interneurons
- **Gray matter interneurons:** *central pattern generators (CPGs)* are here — networks that generate rhythmic stepping patterns (target for locomotor restoration)

- **Key distinction:** dorsal roots carry input *to* spinal motor circuits; dorsal columns carry information *past* them to the brain

Spine Anatomy & Physiology: A Quick Primer

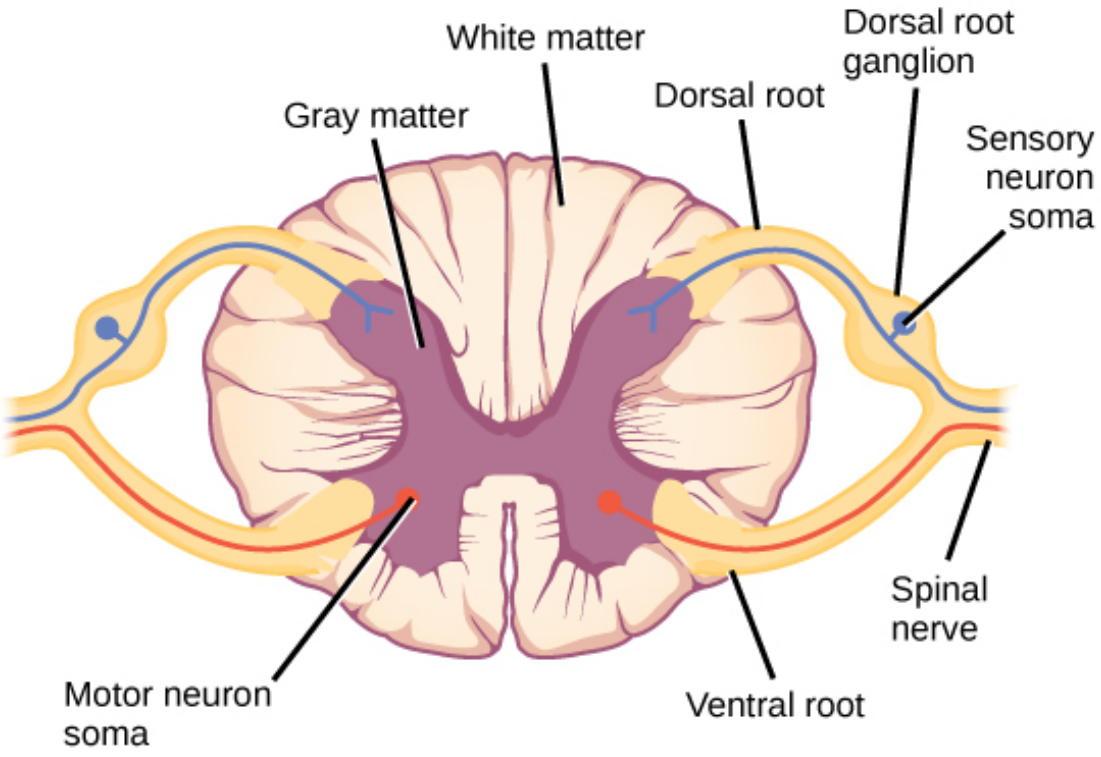

Cross Section of Spinal Cord

Image: [7]

Paradigm Shift: Dosral Column → Dorsal Roots

- 50 years of pain SCS targeted dorsal columns — but never restored locomotion, because dorsal columns are not wired to locomotor circuits

Image: [9]

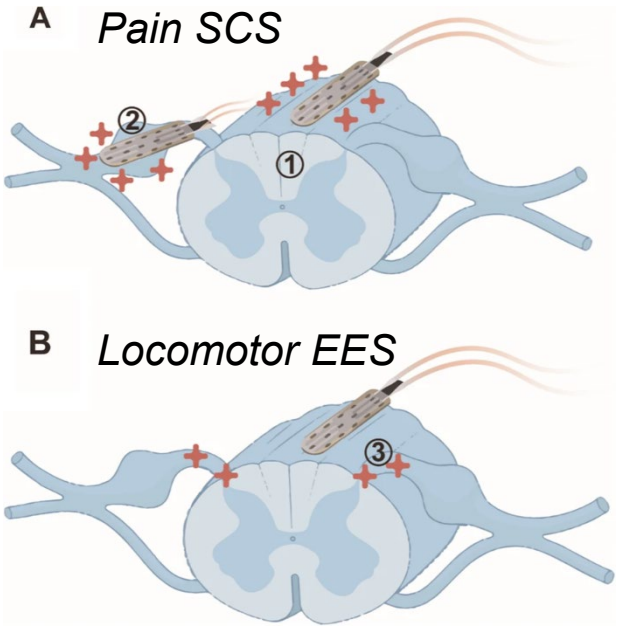

- Courtine & Bloch (EPFL/CHUV) identified a fundamentally different target: **dorsal root proprioceptive afferents** (Ia/Ib/II fibers)

- **Capogrosso et al. (2013)**: 3D FEM + cable model demonstrated that epidural currents preferentially recruit dorsal root afferents at lower thresholds than dorsal columns due to CSF shunting and root geometry [3]
  - Computational confirmation (in Sim4Life) that clinical epidural SCS preferentially activates the functionally correct target (dorsal roots) provided the biophysical foundation for the STIMO program

- **Formento et al. (2018)**: continuous EES causes "transient deafferentation" in humans [4]
  - Mechanism: antidromic action potentials collide with incoming proprioceptive signals; refractory period occupation further jams the afferents
  - Humans (unlike rats) depend heavily on real-time proprioceptive feedback for locomotion so continuous stimulation is catastrophic
  - Solution: spatiotemporal patterning delivers brief, phase-appropriate bursts, leaving afferents free to carry natural feedback between stimulation windows

Outline for Today

- SCS History: Gate control to modern paradigms
- **Biophysics: Dorsal column vs. dorsal root recruitment**
- STIMO Breakthrough: Clinical results & translation
- Personalized Pipeline: The STIMO-2 case study
- Exposure Safety: LF limits, MRI safety, implant considerations

Spinal Cord Electrical Properties

IT'IS Tissue Property Database

- **CSF:** σ ≈ 1.8 S/m — highest conductivity in the spinal canal; preferential current pathway from electrode to root entry zones [3], [16]
- **Epidural fat:** σ ≈ 0.04 S/m: low-conductivity insulator between electrode and dura
- **White matter:** anisotropic: σ_long ≈ 0.1 S/m, σ_trans ≈ 0.01 S/m [16]; current propagates along fiber tracts but penetrates poorly from dorsal surface into the cord
- **Gray matter:** σ ≈ 0.23 S/m, isotropic [16]: but shielded behind low-transverse-conductivity white matter; EES cannot directly depolarize interneurons or motoneurons even at 600 µA [3]
- **Dorsal CSF thickness** is the dominant geometric variable [8]; typical inter-patient variation is significant (> 2x) → drives the need for patient-specific modeling (Part 5)
- **Result:** epidural current flows laterally through CSF, reaching dorsal root afferents at entry-zone bends at far lower thresholds than dorsal column fibers or gray matter cells [3]
- All properties from IT'IS tissue database [16], built on the Gabriel measurement series [46]–[48]

Why Current Flows Where It Does

Capogrosso et al. 2013

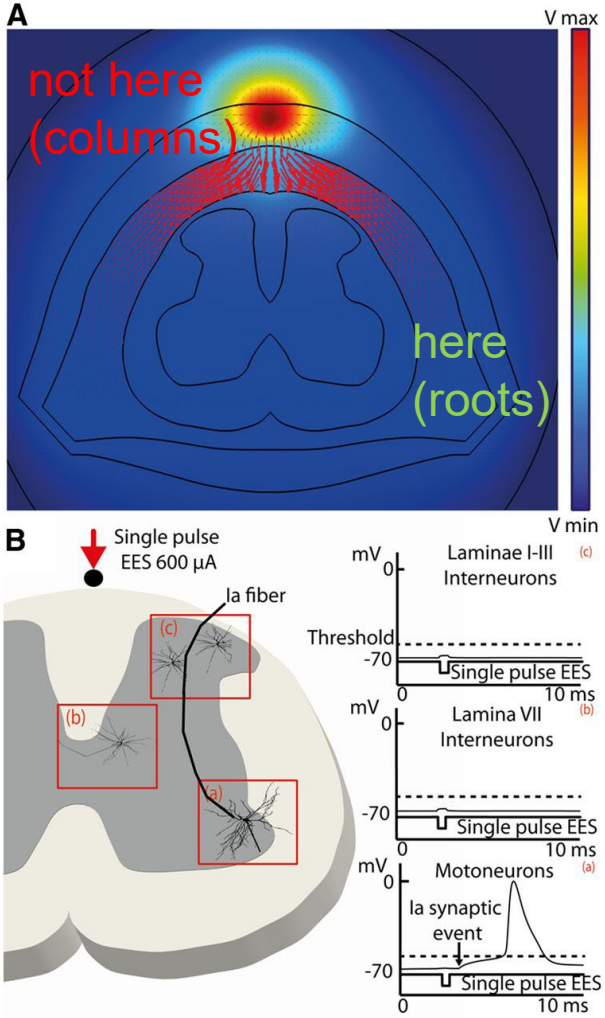

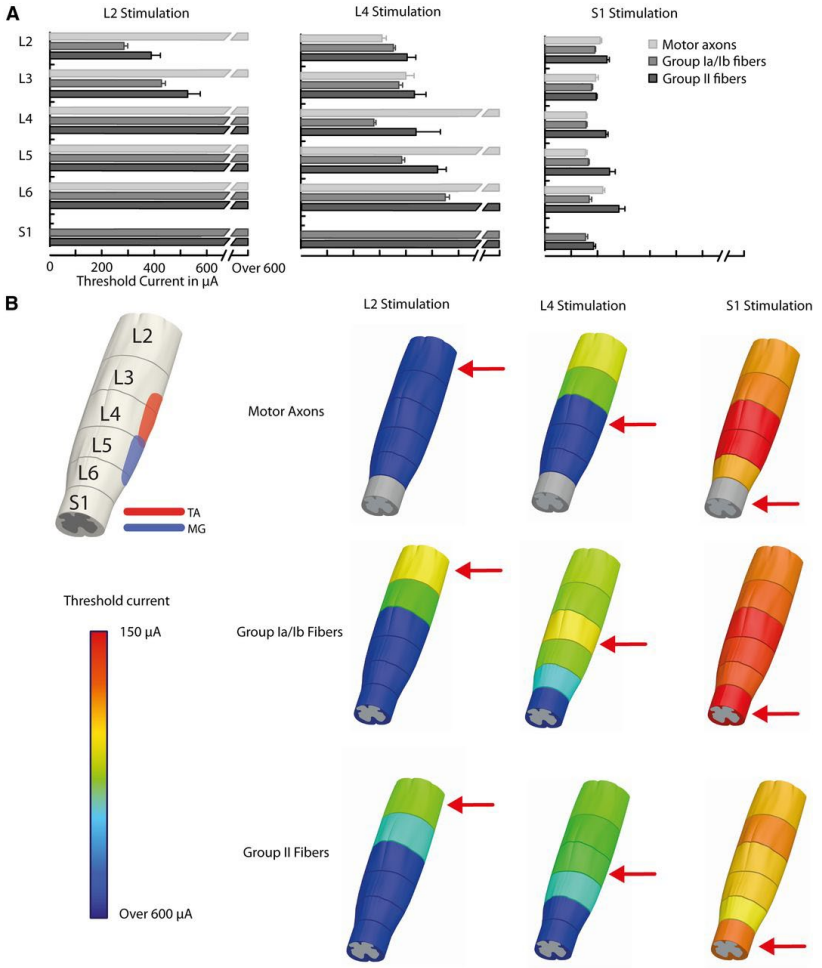

Image: [8]

Dorsal Roots Recruited First

Recruitment Order Driven By…

1. Current Distribution

- High-conductivity CSF preferentially channels current toward root entry zones [3], [34]
- Dorsal column fibers, though geometrically close to the electrode, are shielded within low-transverse-conductivity white matter [29]

2. Geometry → Activating Function

- Dorsal root fibers *curve sharply* as they enter the cord → large $\partial^2 V_e/\partial x^2$ at bending points [7], [30]
- Dorsal column fibers run longitudinally → relatively uniform $\partial^2 V_e/\partial x^2$ → higher thresholds
- Recall: activating function f(x) = $\partial^2 V_e/\partial x^2$ is the cable-equation forcing term (W3, EN) [7]

3. Fiber Properties

- Large-diameter proprioceptive afferents in roots (Ia: 13–20 µm) have lower thresholds than smaller dorsal column fibers due to greater internodal spacing [31], [32]

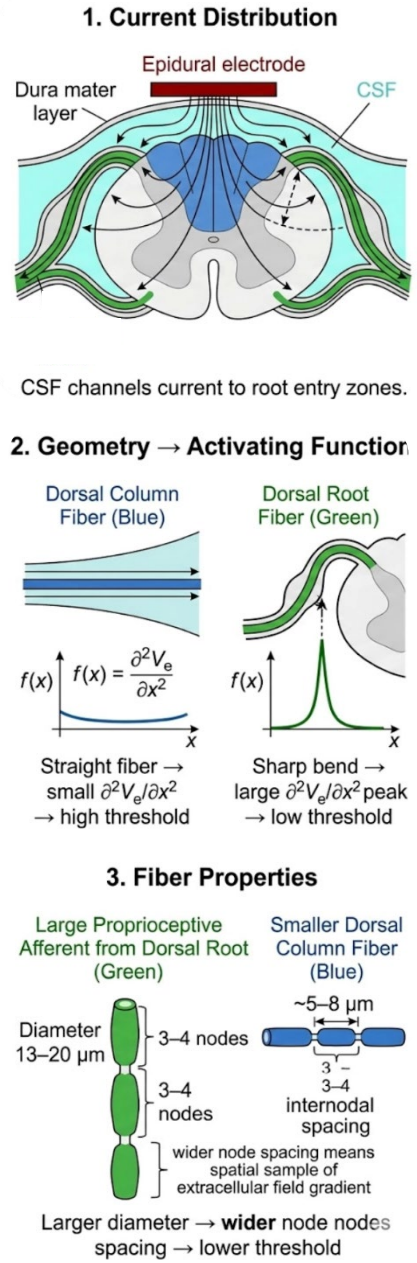

Image: [10]

Holsheimer's Computational SCS Models

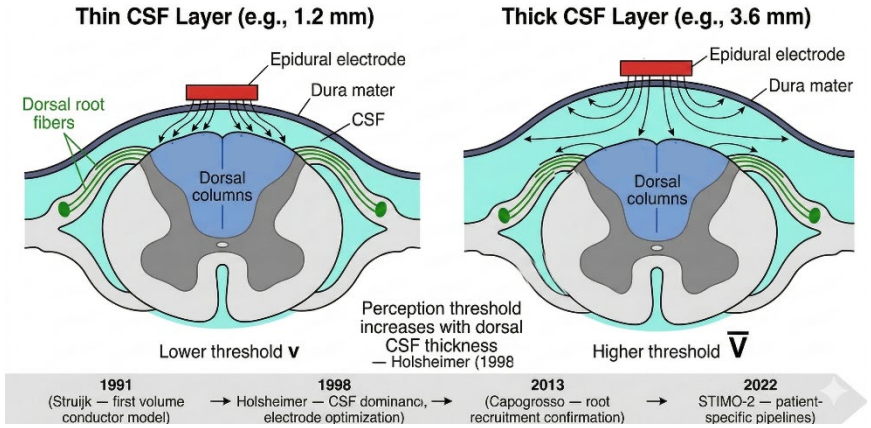

Image: [11]

- Struijk, Holsheimer & Boom (1991): first detailed volume conductor model of epidural SCS using inhomogeneous, anisotropic geometry [29]
- **Key finding:** dorsal CSF thickness is the dominant geometric factor — threshold varies strongly with CSF layer depth [8]

- Holsheimer (1998): narrow bipole and transverse tripole configurations optimize selectivity between dorsal column and dorsal root activation [9]
- Holsheimer & Wesselink (1997): narrow contacts and transverse tripolar configurations maximize the DC/DR threshold ratio, improving the therapeutic window [33]
- **Legacy:** established that computational optimization of electrode geometry could substantially improve clinical outcomes — a principle now extended to locomotor SCS
- These models laid the computational groundwork 30 years before patient-specific pipelines became feasible

Why Dorsal Roots Have Lower Thresholds

- **Straight dorsal column fibers:** run longitudinally through a slowly varying field → small $f(x) = \partial^2 V_e/\partial x^2$ (AF) peaks → high thresholds
- **Curving dorsal root fibers:** sharp bend at the root entry zone creates a large spatial derivative even in moderate fields [30], [34]
  - Result: AF peaks strongly at the bend point → low thresholds
- Struijk et al. (1993): computational models confirmed that root fibers at entry-zone bends are activated at 30–50% lower amplitude than parallel dorsal column fibers at the same distance [30]
- This is the quantitative explanation behind the three qualitative explanations on slide 20 — geometry is the dominant factor

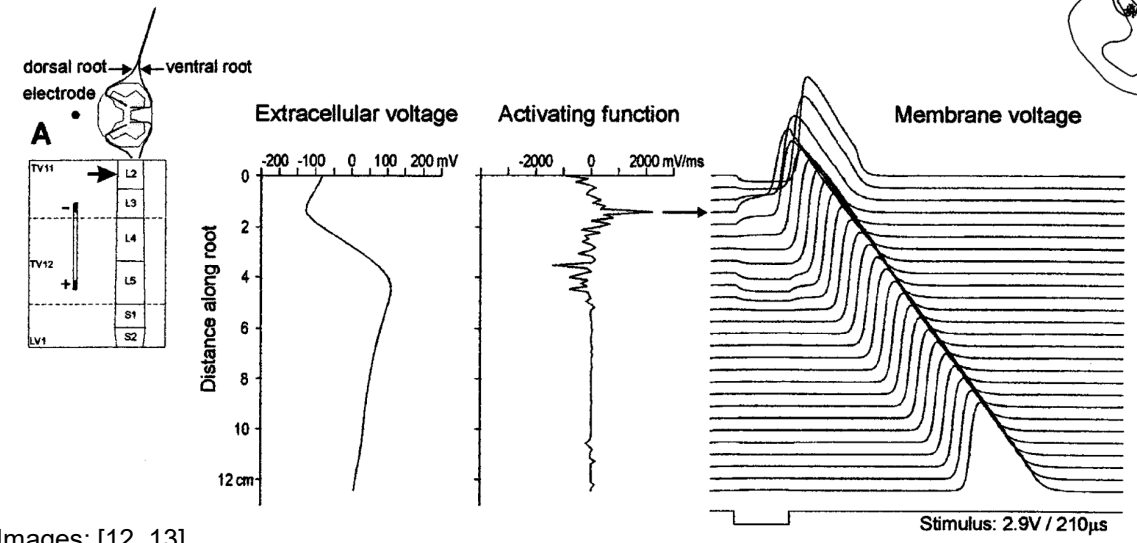

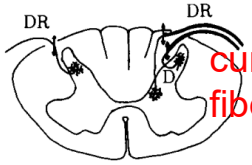

linear column fibers

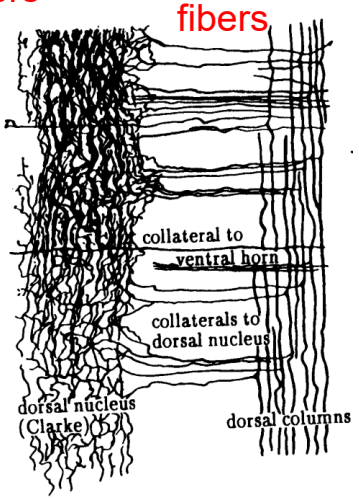

Images: [12, 13]

Spatiotemporal Patterning

- Motoneuron pools in the lumbosacral cord are organized somatotopically — each dorsal root entry zone maps to specific muscle groups [36]
- EMG recordings during locomotion → back-projection onto spinal segments identifies which rootlets activate during each gait phase [37]
- **Gait phases and motor targets:**
  - Propulsion (push-off): extension-related roots — gastrocnemius, soleus
  - Weight acceptance (early stance): stability-related roots — vastus lateralis, gluteus
  - Swing (leg advance): flexion-related roots — iliopsoas, tibialis anterior
- Spatiotemporal EES delivers stimulation to specific root entry zones with timing matched to the natural activation sequence [5]
- Formento et al. (2018): continuous (non-patterned) EES causes “transient deafferentation” — blocks proprioception in humans [4]
  - Spatiotemporal patterning avoids this by providing only brief, phase-appropriate bursts

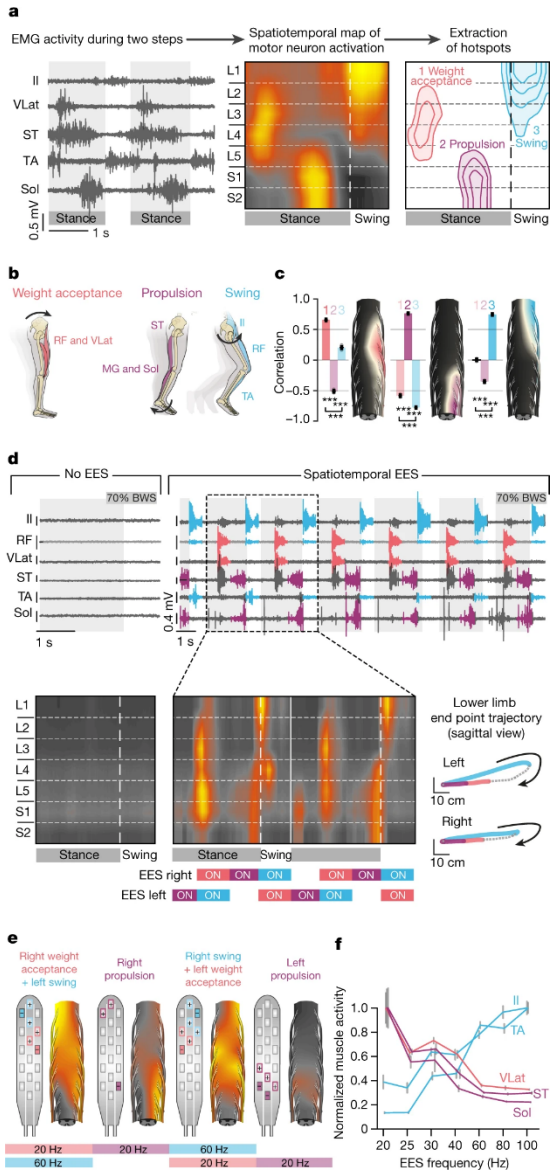

Image: [14]

Outline for Today

- SCS History: Gate control to modern paradigms
- Biophysics: Dorsal column vs. dorsal root recruitment
- **STIMO Breakthrough: Clinical results & translation**
- Personalized Pipeline: The STIMO-2 case study
- Exposure Safety: LF limits, MRI safety, implant considerations

Targeted Neurotech Restores Walking (STIMO)

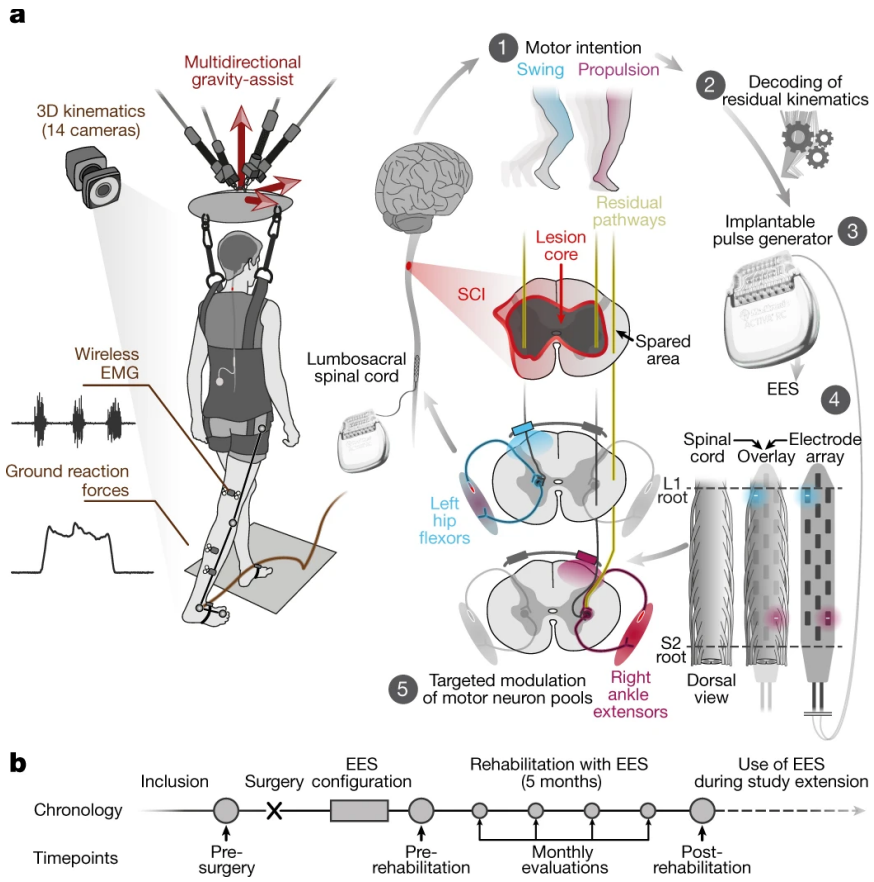

Image: [14]

- First-in-human trial (NCT02936453) of spatiotemporally patterned EES [5]
- **3 individuals** with chronic SCI (>4 years post-injury); permanent motor deficits or complete paralysis
- Spatiotemporal stimulation: within **one week**, adaptive control of paralyzed muscles re-established during overground walking [5]
- After several months of rehabilitation with EES: voluntary control over previously paralyzed muscles recovered **even without stimulation** — activity-dependent neuroplasticity [5]
- Companion paper: Formento et al. (2018) — computational rationale establishing dorsal roots as the therapeutic target [4]

Paralysis Recovered In One Day (STIMO-2)

- **3 individuals** with complete sensorimotor paralysis (AIS-A), including complete loss of sensation in 2 participants [6]
- Custom **16-electrode paddle lead** designed using patient-specific computational modeling to target dorsal root ensemble for leg and trunk motor neuron pools [6]
- Within **a single day** of activation: standing, walking, cycling, swimming, and trunk control restored [6]
- After 3–4 months neurorehabilitation: standing 2 h, walking 500 m independently, climbing stairs [6]
- **Critical precision requirement:** 2 mm displacement from computationally predicted optimal position → measurable selectivity loss [6]

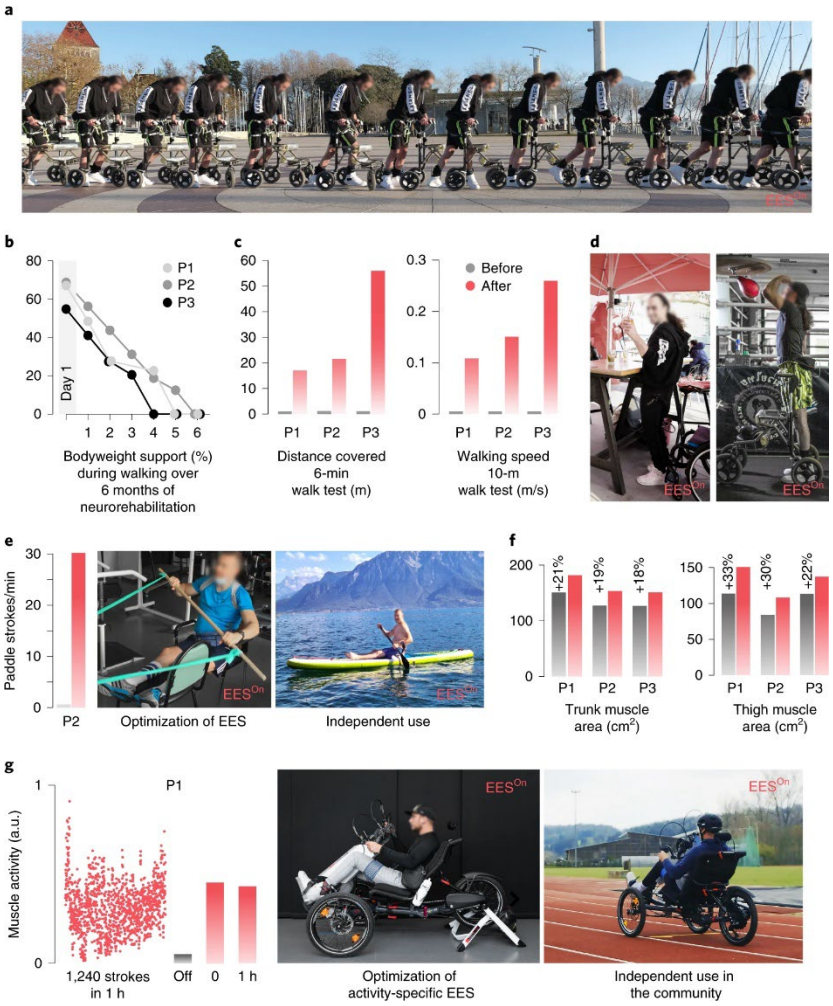

Image: [15]

SCVsx2::Hoxa10 Neurons Restore Walking

- Kathe et al. (2022): identified the specific neuronal subpopulation orchestrating recovery under EES-assisted rehabilitation in mice [38]
- **SCVsx2::Hoxa10 neurons**: excitatory interneurons in the lumbar spinal cord expressing Vsx2 [38]
- Techniques: single-nucleus RNA sequencing + spatial transcriptomics + activity-dependent genetic labeling
- **Counterintuitive finding:** recovery involved a **reduction** in overall neuronal activity during walking — reflecting activity-dependent selection of essential relay neurons [38]
- Significance: understanding which neurons mediate recovery could guide next-generation stimulation strategies and targeted molecular therapies
- Note: this paper addresses **recovery mechanisms and circuit reorganization**, not stimulation engineering itself

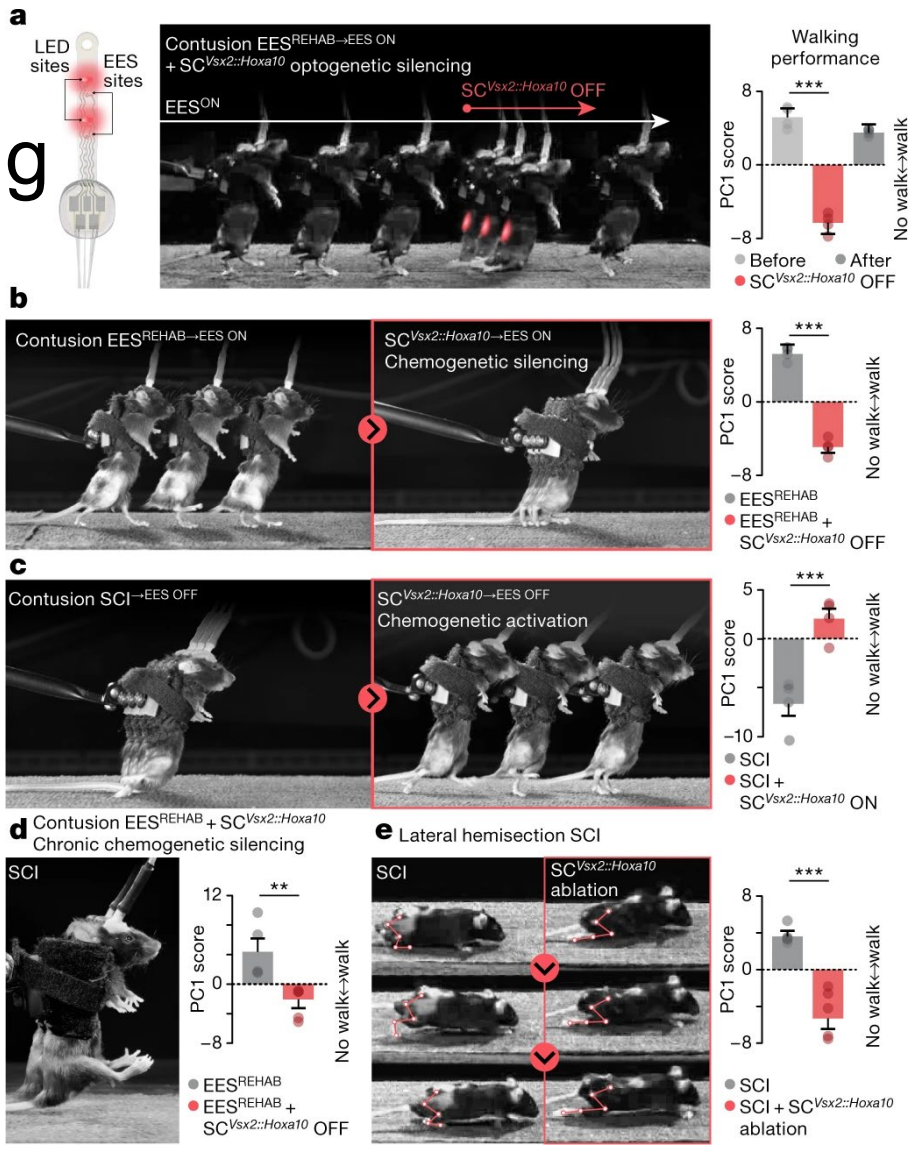

Image: [16]

Beyond STIMO: 2023–2025

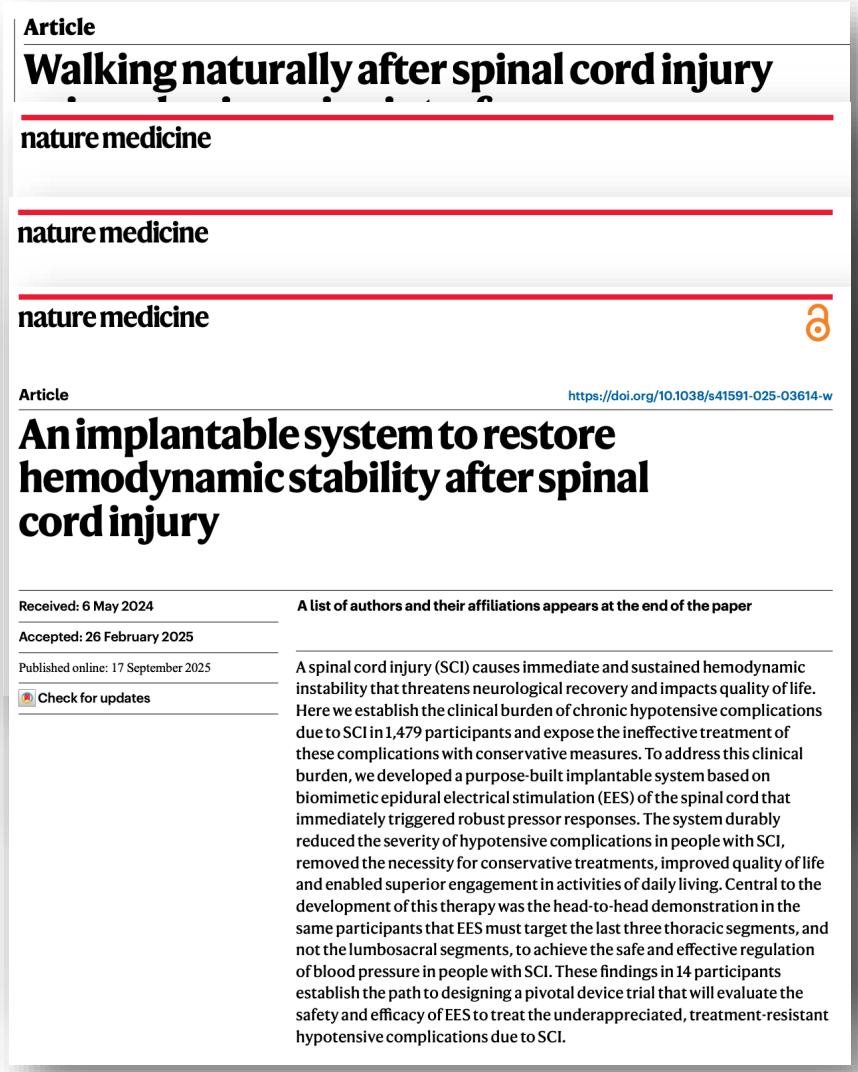

Article

Walking naturally after spinal cord injury

nature medicine

nature medicine

nature medicine

Article

https://doi.org/10.1038/s41591-025-03614-w

An implantable system to restore hemodynamic stability after spinal cord injury

Received: 6 May 2024

Accepted: 26 February 2025

Published online: 17 September 2025

Check for updates

A list of authors and their affiliations appears at the end of the paper

A spinal cord injury (SCI) causes immediate and sustained hemodynamic instability that threatens neurological recovery and impacts quality of life. Here we establish the clinical burden of chronic hypotensive complications due to SCI in 1,479 participants and expose the ineffective treatment of these complications with conservative measures. To address this clinical burden, we developed a purpose-built implantable system based on biomimetic epidural electrical stimulation (EES) of the spinal cord that immediately triggered robust pressor responses. The system durably reduced the severity of hypotensive complications in people with SCI, removed the necessity for conservative treatments, improved quality of life and enabled superior engagement in activities of daily living. Central to the development of this therapy was the head-to-head demonstration in the same participants that EES must target the last three thoracic segments, and not the lumbosacral segments, to achieve the safe and effective regulation of blood pressure in people with SCI. These findings in 14 participants establish the path to designing a pivotal device trial that will evaluate the safety and efficacy of EES to treat the underappreciated, treatment-resistant hypotensive complications due to SCI.

- **Brain-spine interface** (Lorach et al., Nature 2023): 1 participant with chronic tetraplegia; wireless cortical-to-spinal decoding enabled natural walking, stair climbing, complex terrain; interface stable >1 year [39]
- **Parkinson's disease** (Milekovic et al., Nat. Med. 2023): spinal cord neuroprosthesis improved locomotor deficits in primates and humans — extending SCS beyond SCI [40]
- **Hypothalamic DBS** (Cho et al., Nat. Med. 2024): DBS of lateral hypothalamus augmented walking in 2 humans with incomplete SCI [41]
- **Hemodynamic restoration** (Phillips et al., Nat. Med. 2025): implantable EES restored blood pressure stability in 14 patients, 4 clinical studies [42]
- **Trajectory:** single-application pain relief → multi-indication neuroprosthetic platform

ONWARD Medical

Image: [17]

- Founded 2014 as G-Therapeutics, later GTX Medical, now ONWARD Medical (EPFL spin-off); co-founders: Courtine & Bloch [43]
  - IPO on Euronext Brussels, Oct 2021; raised €75.2m gross
- **ARC-EX** (transcutaneous): upper-limb function in cervical SCI [44]
  - Up-LIFT trial: 65 participants, 72% responder rate [44]
  - FDA De Novo: Dec 2024 — first FDA-cleared non-invasive SCS for SCI
  - CE Mark: Sept 2025
- **ARC-IM** (implantable): autonomic (blood pressure) + mobility indications [42]
  - FDA IDE approval: Aug 2025 (Empower BP pivotal study)
  - First patient enrolled: Feb 2026
- **ARC-BCI** (brain-computer interface): ARC-IM + WIMAGINE cortical BCI (CEA-Clinatec); 5 implanted through mid-2025 [39]
- Patent portfolio: >150 issued (>290 incl. European validations)

ONWARD™
EMPOWERING MOVEMENT™

SCS Landscape Overview (2026)

	Pain SCS	Locomotor EES	Emerging
Target	Dorsal columns/DRG	Dorsal root afferents	BCI, autonomic, PD
Pattern	Continuous/burst/ HF10	Spatiotemporal, activity-specific	Intent-driven, closed-loop
Personalization	Beneficial	**Essential** (2 mm sensitivity)	Essential
Modeling role	Design guidance	Clinical-grade pipeline	Enabling infrastructure
Scale	~50k implants/yr	Implantable system in trials	First-in-human

Outline for Today

- SCS History: Gate control to modern paradigms
- Biophysics: Dorsal column vs. dorsal root recruitment
- STIMO Breakthrough: Clinical results & translation
- **Personalized Pipeline: The STIMO-2 case study**
- Exposure Safety: LF limits, MRI safety, implant considerations

Why Personalization is Needed

Personalization & Inter-Individual Variability

- Significant inter-patient variation in:
  - Spinal cord cross-sectional area and position within the canal
  - CSF layer thickness and distribution
  - Dorsal root entry zone positions relative to vertebral landmarks
  - Vertebral dimensions and curvature
- Holsheimer: CSF thickness alone shifts activation thresholds meaningfully [8], [29]; CSF thickness varies by > 2x across subjects [63]

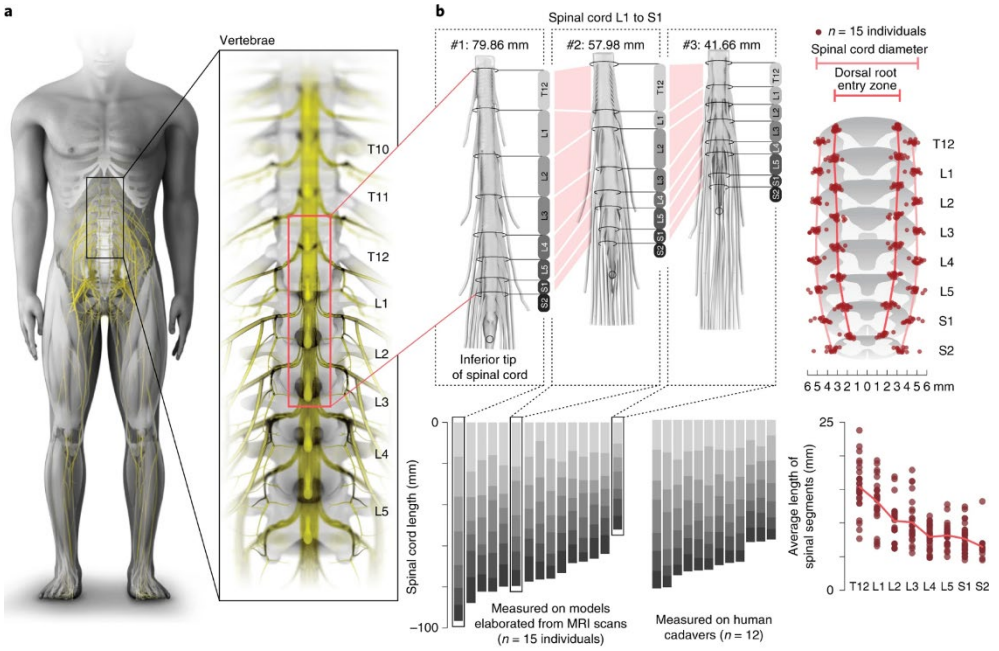

- Same lead position → **different** recruitment patterns in different patients
- Rowald et al. (2022): 2 mm displacement from optimal position → measurable selectivity loss [6]
- **Conclusion:** one-size-fits-all approaches are insufficient — patient-specific modeling is not optional for locomotor SCS

Image: [18]

STIMO-2 Personalized Planning Pipeline

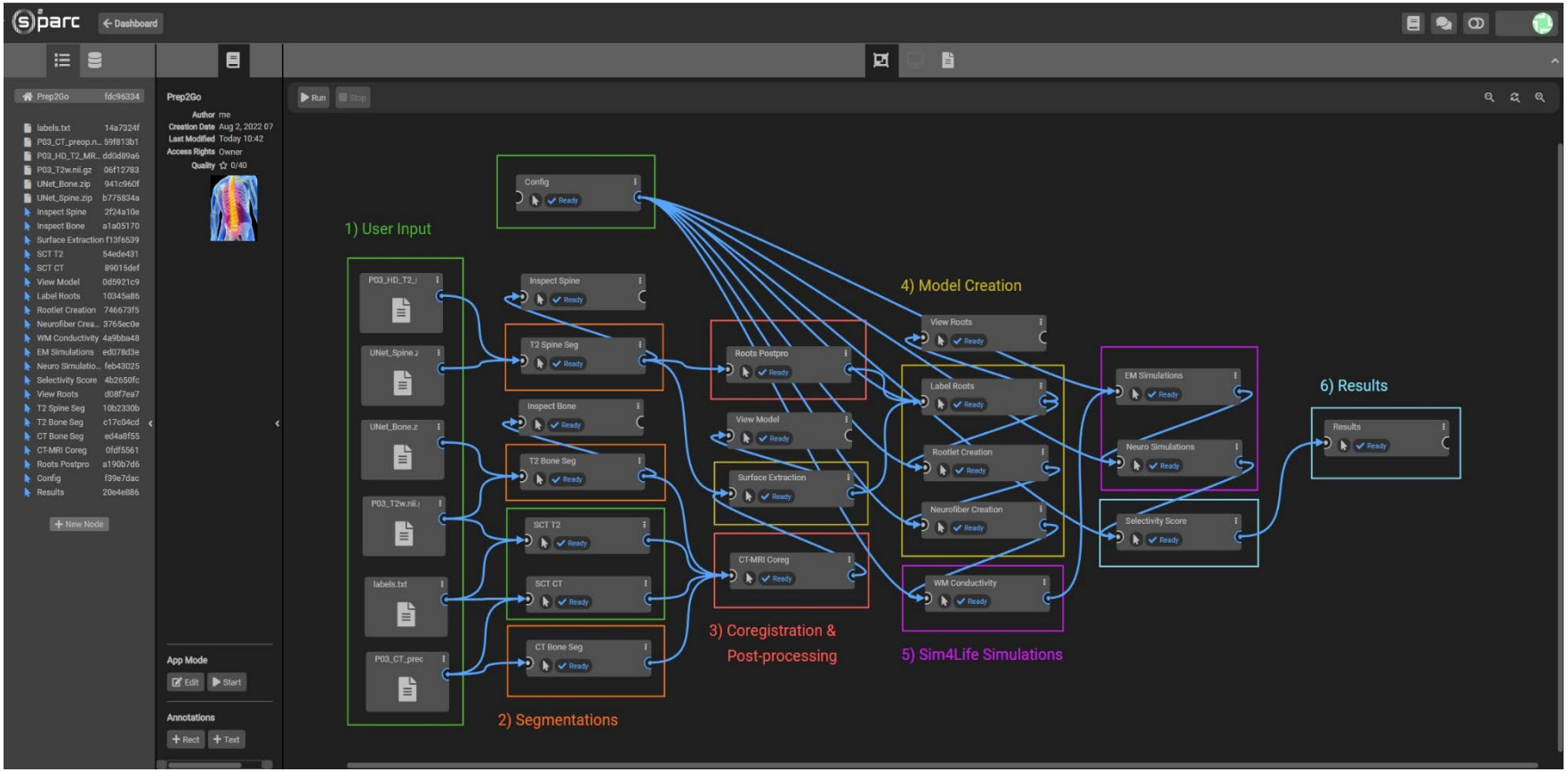

MRI → Surgical Plan: Pipeline

1. Planning & setup (GUI)

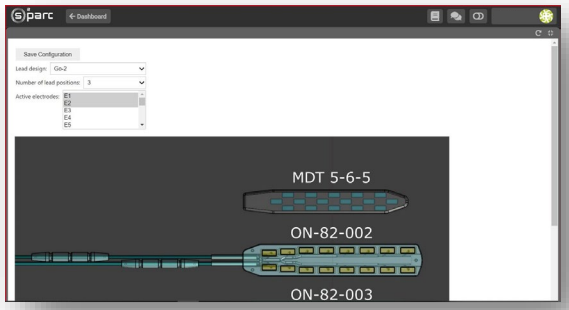

2. AI segmentation inspect & correct

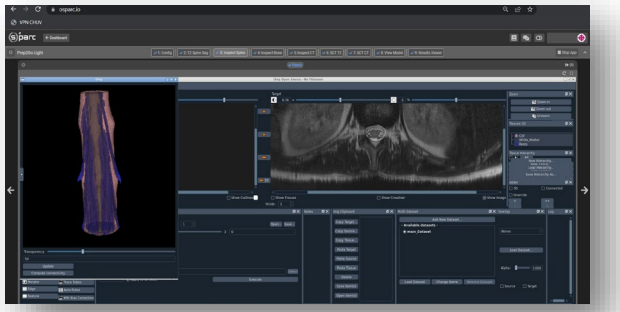

3. Vertebrae selection (CT co-reg)

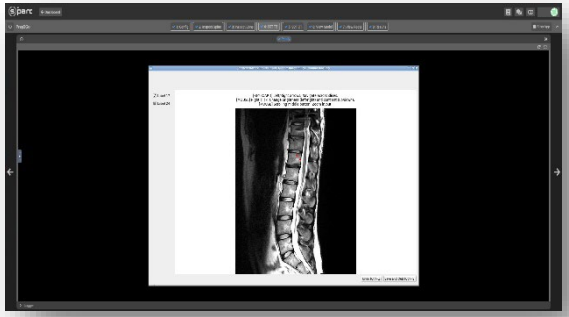

4. S4L:web model inspection

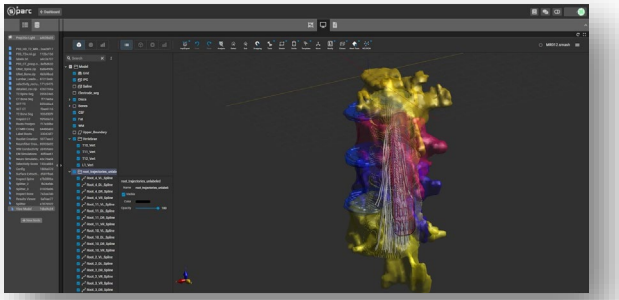

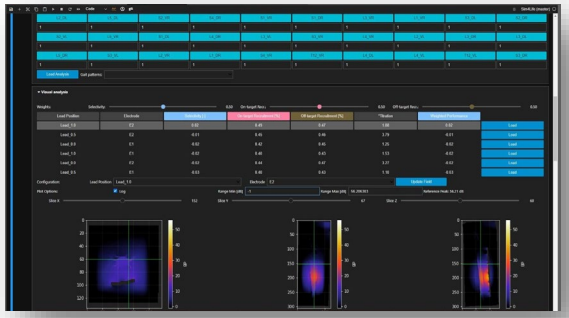

5. Results: analysis, decision making, report (pdf)

Lead Design: Paddle vs. Percutaneous

- **Percutaneous leads:** cylindrical, inserted via Tuohy needle (minimally invasive); 4–8 contacts in linear array; higher migration rates
- **Paddle leads:** flat, surgically placed via laminotomy; 8–32 contacts in 2D arrays; lower migration, broader coverage, better energy efficiency
- **North et al. (2005) RCT:** 83% paddle vs. 42% percutaneous success at 1.9 years ($p < 0.05$) [49]
- **For locomotor SCS:** Rowald et al. custom 16-electrode paddle designed via computational optimization to cover the target dorsal root ensemble [6]
- **Holsheimer design principles:** narrow bipole / transverse tripole configurations optimize DC/DR selectivity [9], [33]
  - Building on the electrode design trade-offs (selectivity, efficiency, safety) from W5 (EN)
- **Key design parameters:** contact size (width, length), inter-contact spacing, contact count, lead width, curvature to match spinal canal anatomy

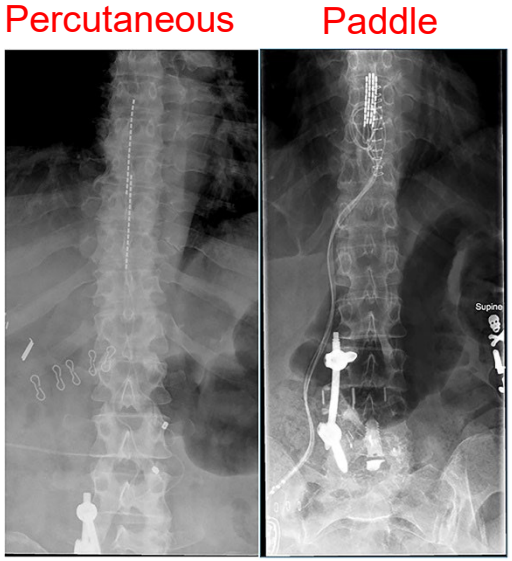

Image: [19]

Boston Scientific Lead Designs

Image: [20]

From Pipeline to Clinical Outputs

- **GAF acceleration:** the generalized activating function (W3, EN) applied in 3D patient-specific context provides ~10^3 speedup over full NEURON titration [50]
  - Enables real-time exploration of the high-dimensional configuration space (16 contacts × amplitude × timing)
- **Optimization outputs** (general methods covered in W11, EN):
  - Optimal electrode configurations per target muscle group
  - Stimulation timing sequences matched to gait phases
  - Pareto trade-off curves: selectivity vs. amplitude vs. off-target |activation
- **Clinical deliverables:**
  - PDF surgical planning report: recommended paddle placement, contact assignments
  - Initial stimulation programs ready for intraoperative testing
  - Cloud deployment via o2S2PARC [52] enables pipeline use in clinical settings without local HPC
- **Goal:** reduce pre-operative planning from months to <24 hours

Outline for Today

- SCS History: Gate control to modern paradigms
- Biophysics: Dorsal column vs. dorsal root recruitment
- STIMO Breakthrough: Clinical results & translation
- Personalized Pipeline: The STIMO-2 case study
- **Exposure Safety: LF limits, MRI safety, implant considerations**

Therapeutic Recruitment vs. Unintended Stimulation

- **SCS:** deliberately maximize recruitment of target neural elements (dorsal root afferents) while minimizing off-target activation
- **Exposure safety:** prevent any unintended nerve or muscle stimulation from external or implant-related electromagnetic fields

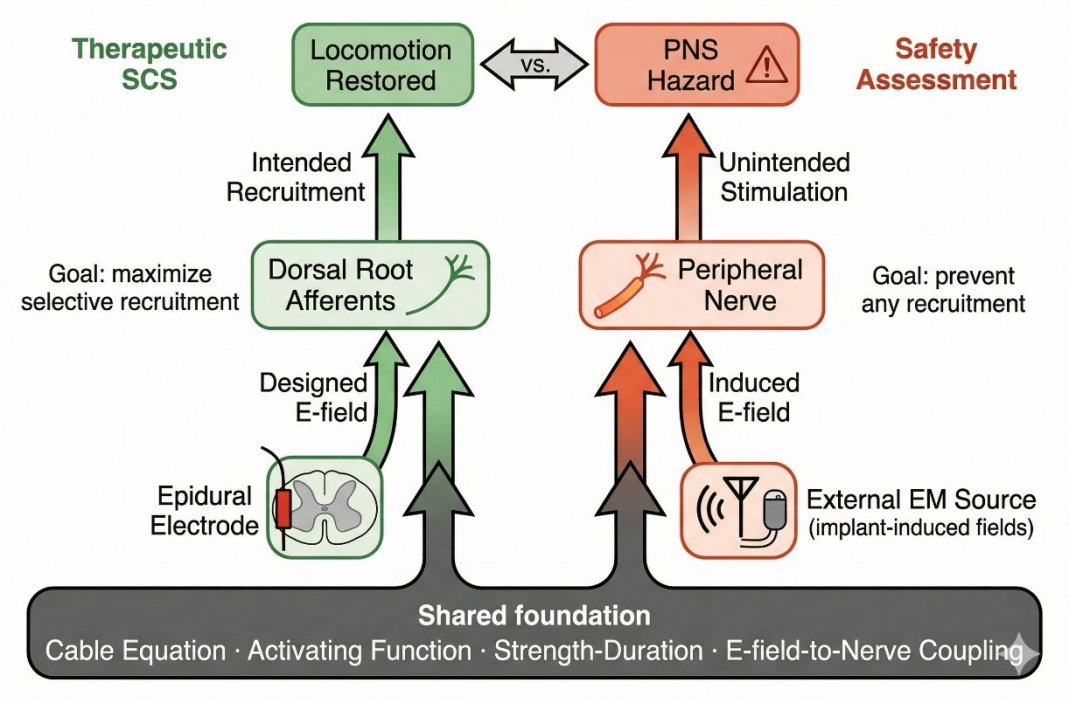

Image: [21]

- **The important biophysical mechanisms are the same:**
  - Cable equation dynamics
  - Strength-duration relationships
  - Activating function analysis
  - E-field-to-nerve coupling
- **Same tools:** IT'IS uses the Sim4Life T-NEURO platform and Virtual Population models for both therapeutic optimization and safety assessment [45]
- **Practical implication:** Fields optimized for (beneficial) SCS become a hazard when they unintentionally recruit nerves near implants — quantifiable limits needed

Rheobase and Chronaxie

- **Weiss-Lapicque relationship** [53, 54]:
$$I_{th} = I_{rh}\left(1 + \frac{\tau_{ch}}{PW}\right)$$
- **Rheobase** (I_{rh}): minimum current for excitation at infinite pulse duration
- **Chronaxie** (τ_{ch}): pulse width where threshold = 2× I_{rh}
  - Myelinated peripheral nerves: τ_{ch} ≈ 30–200 µs [55]
  - Cardiac muscle: τ_{ch} ≈ 1–3 ms (much longer — hence high-frequency fields are less cardiotoxic)
- Larger-diameter, myelinated fibers → lower rheobase, shorter chronaxie → recruited first [31]
  - Same principle as in SCS dorsal root targeting

- For time-varying (sinusoidal) fields: effective pulse duration ≈ half-period; frequency-dependent thresholds follow from the strength-duration curve
- This relationship underpins **both** SCS pulse programming **and** LF safety standard derivation [10]

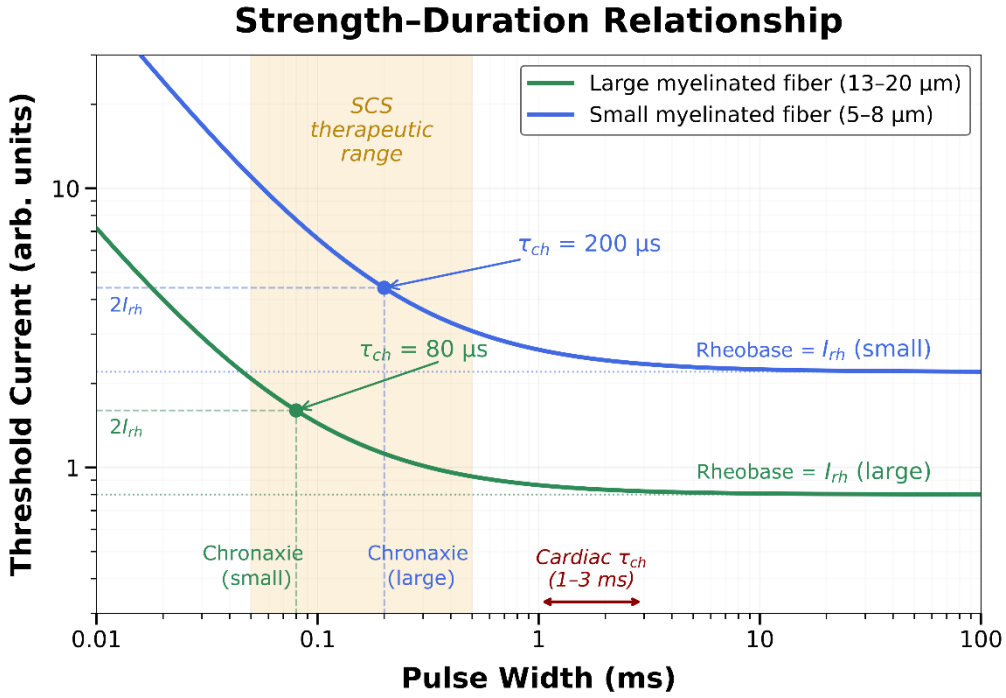

ICNIRP 2010: Low-Frequency Exposure Guidelines

- Replaced 1998 guidelines: **internal induced E-field** (V/m) is the primary dosimetric quantity (replacing current density) [10]
- **Basic restrictions:**
  - CNS (head): 10 mV/m at 10–25 Hz (to prevent magnetophosphenes)
  - PNS (all tissues): frequency-dependent; rising with frequency per the strength-duration relationship
  - **Reference levels:** external field quantities (E in V/m, B in μT) derived from basic restrictions via computational dosimetry in anatomical models [10]

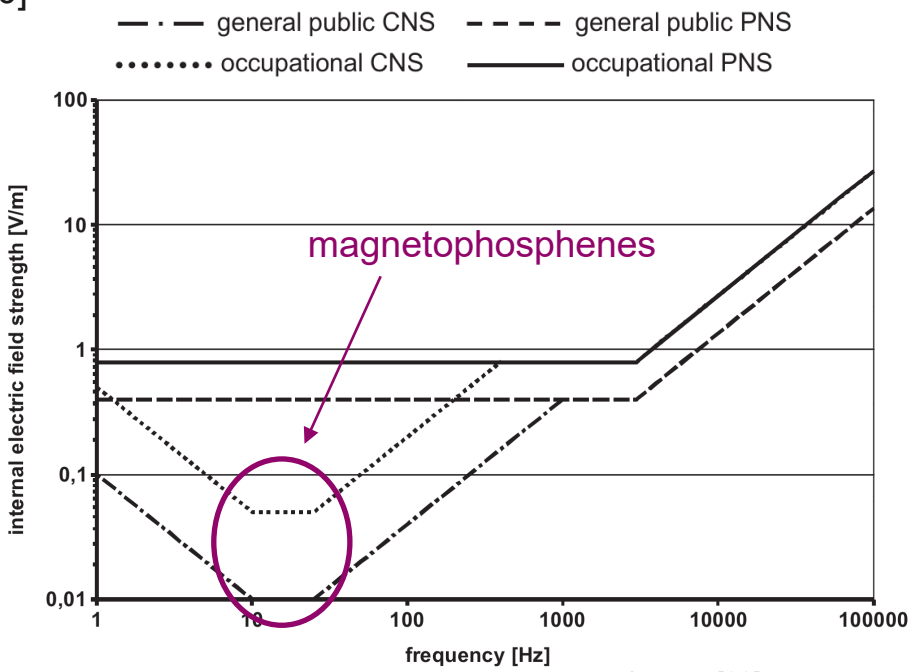

Image: [22]

- Below ~10 Hz: dominant concern → CNS stimulation effects
- 10 Hz – 100 kHz: dominant hazard → **PNS of myelinated nerve fibers** (the same fibers targeted in SCS)
- **IEEE C95.1-2019** provides complementary framework with DRLs and ERLs for restricted/unrestricted environments [11]
- Safety limits derived using strength-duration relationships computed in anatomical models (ViP) with coupled EM-neuro simulations

Computational PNS Prediction with ViP Models

- **Virtual Population (ViP):** 15+ anatomical models covering population diversity [56, 57]
  - Virtual Family (Duke, Ella, Billie, Thelonious) + extended models (Fats, Glenn, pregnant)
  - 80+ tissue types with frequency-dependent properties [16]
- **Neuro-functionalized:** MRG-model axons [14] placed along every major peripheral nerve trajectory — enabling PNS threshold prediction using the coupled EM-neuro workflow from W4 (EN)
- **Population variability drives safety margins:**
  - Ella (thinner body habitus) → lower PNS thresholds
  - Fats (higher BMI) → higher thresholds
  - Safety standards must protect the most sensitive individuals across the population
- **Validation:** Davids et al. (2019) demonstrated that coupled EM-neurodynamic simulations predict MRI gradient PNS thresholds consistent with experimental measurements [58]
- Same ViP models and T-NEURO platform used for both SCS optimization (this lecture) and safety assessment (shared-physics principle)

Image: [22]

Virtual Population

ViP models:

- created from whole-body MRI
- expert/manual segmentation
- 1-2 years to develop model (25+ models)
- level-of-detail determined by target application (e.g., EM safety)
- 110+ tissues characterized (material properties database)
- 280+ PNS structures

Morphed Models

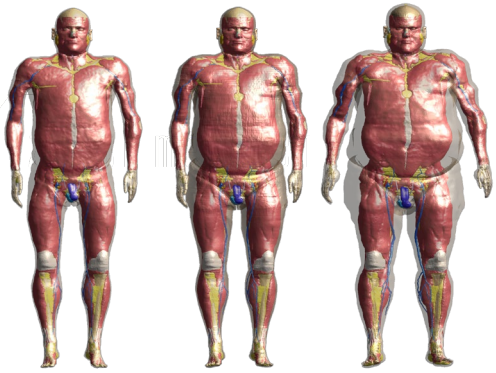

BMI=29 BMI=36 (original) BMI=49

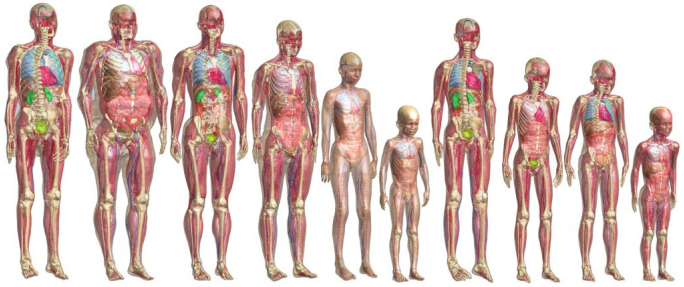

Virtual Population

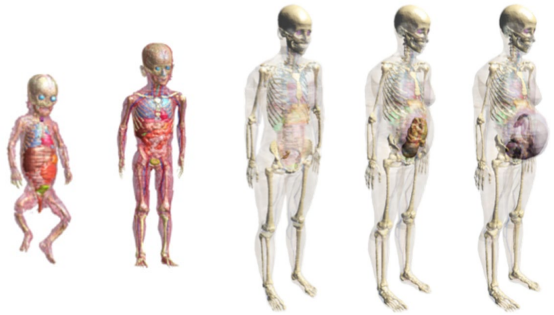

Specific Population

Animal Models

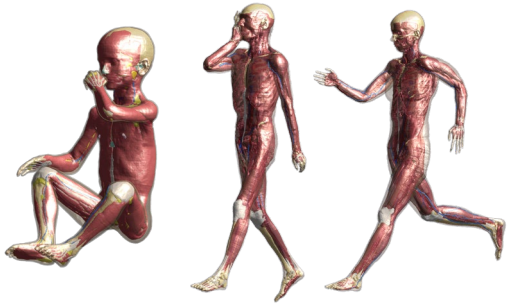

Posed Models

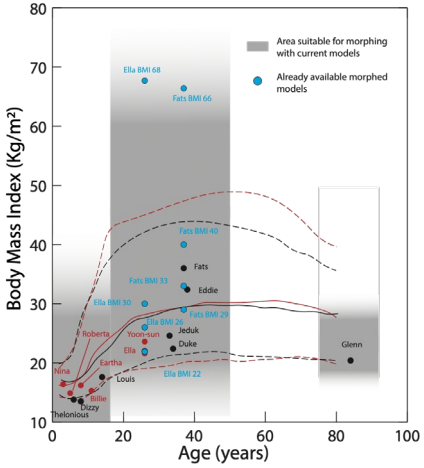

- high-resolution anatomical animal models: the Virtual Zoo (ViZOO); rodent, pig, monkey

NEUROMAN - objectives

- reference computational models for simulating EM-neuron interactions
  - accurate tissue segmentation
  - detailed nerve segmentation and trajectories
  - functionalized for electrophysiology studies in realistic EM fields
- first Asian phantoms for EM exposure simulations, extension of ViP
  - female: Yoon-sun
  - male: Jeduk
- first whole-body monkey phantom
  - female rhesus macaque
  - segment tissues in whole body
  - create neuro-functionalized model

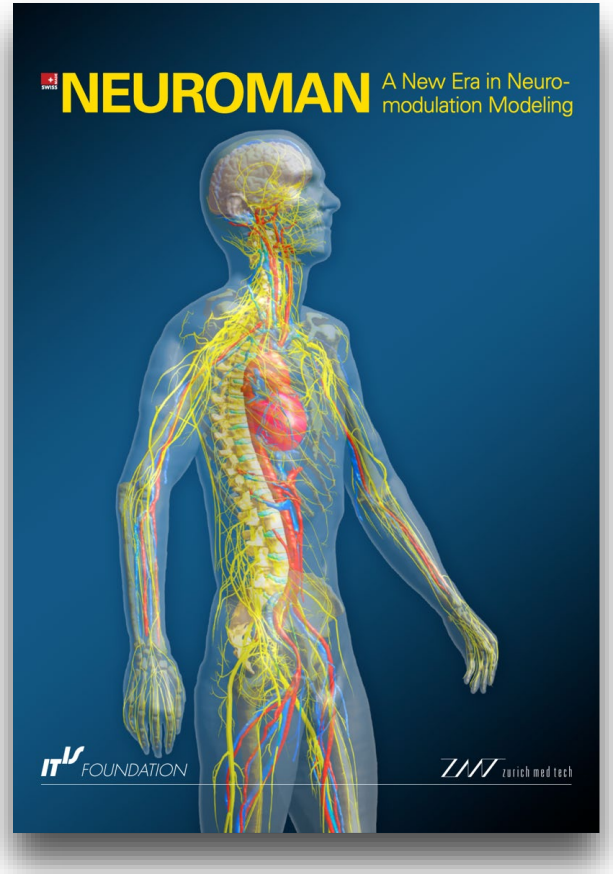

From Visible Korean Data to NEUROMAN Models

- detailed segmentation of tissues and peripheral nerves from Visible Korean Human Project
- high resolution cryosection images of frozen cadavers
  - female: 0.1 x 0.1 x 0.2-1 mm
  - male: 0.2 x 0.2 x 0.2 mm
  - monkey: 0.024 x 0.024 x 0.05-0.5 mm (newly acquired)
- manual and semi-automatic segmentation, with iSeg
  - (github.com/ITISFoundation/osparc-iseg)

Yoon-sun

- Korean female, 26y, 1.52m, 55kg
- Yoon-sun V3 released in July 2018
  - ViP-like: same tissue list as ViP V3.x (> 300)
  - detailed peripheral nerves
  - detailed arteries and veins
  - posable
- neuro-functionalized Yoon-sun V4 released in December 2018
  - contains > 1100 tissues
  - nerves, muscles, arteries and veins separately named and meshed
  - nerve trajectories with default neuron physiology assigned
  - posable

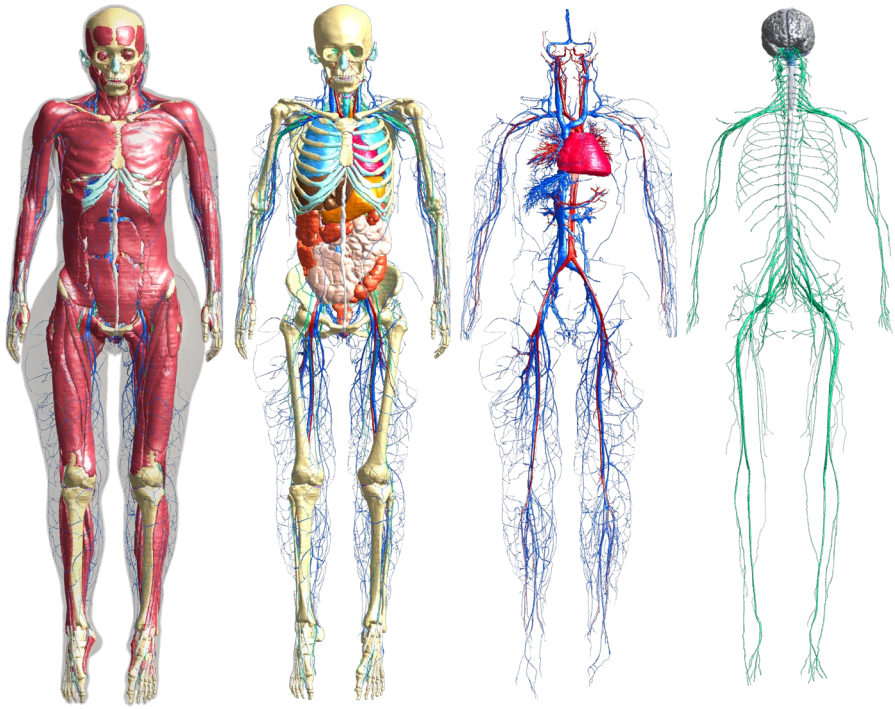

Jeduk

- Korean male, 33y, 1.64m, 55kg
- Jeduk V3 released in March 2019
  - ViP-like: same tissue list as ViP V3.x (> 300)
- same level of detail as Yoon-sun V3
  - detailed peripheral nerves
  - detailed arteries and veins
  - posable
- neuro-functionalized Jeduk V4 released in July 2019
  - contains > 1100 tissues
  - nerves, muscles, arteries and veins separately named and meshed
  - nerve trajectories with default neuron physiology assigned
  - posable

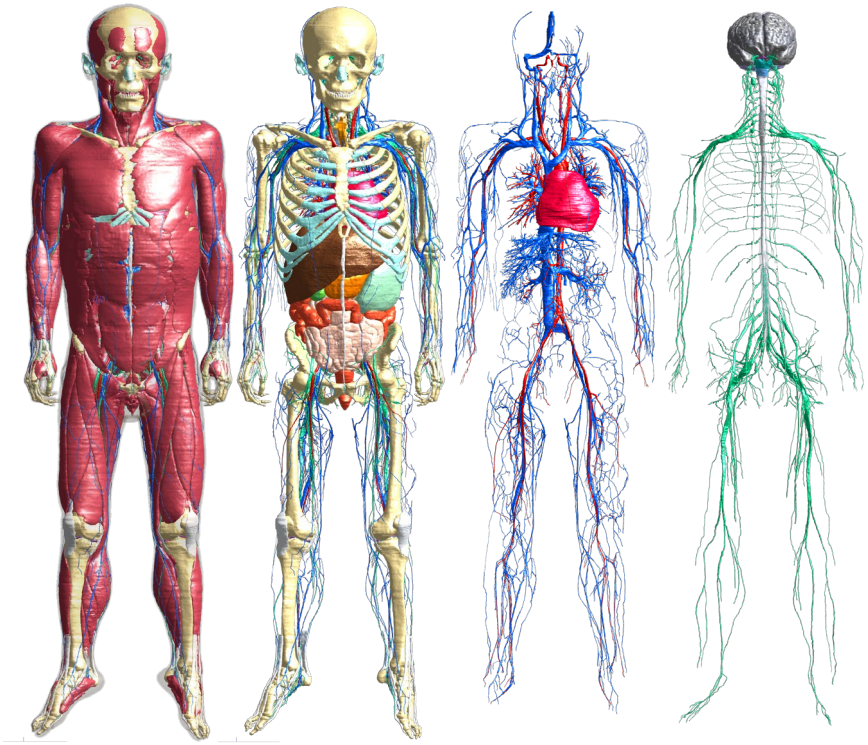

PNS Functionalization

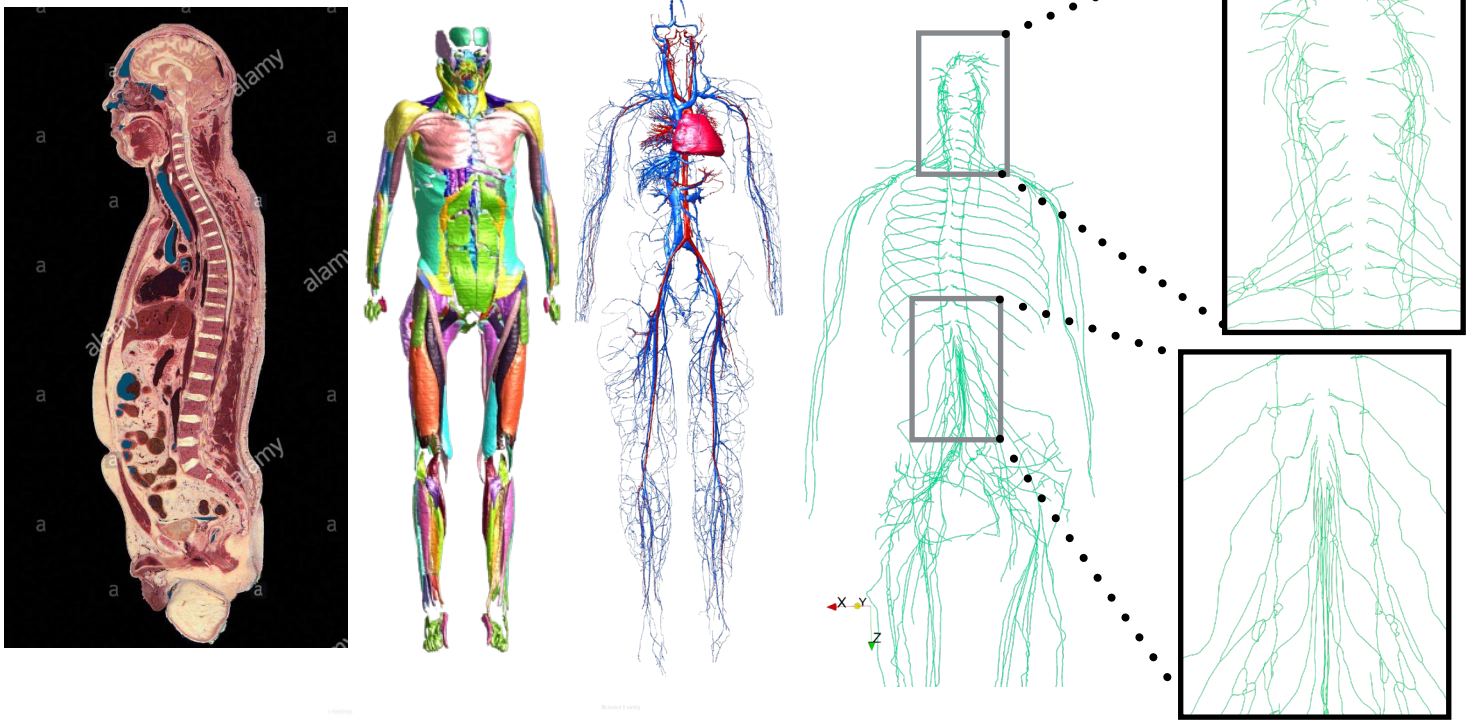

Predicted Stimulation Thresholds (Slew Rate)

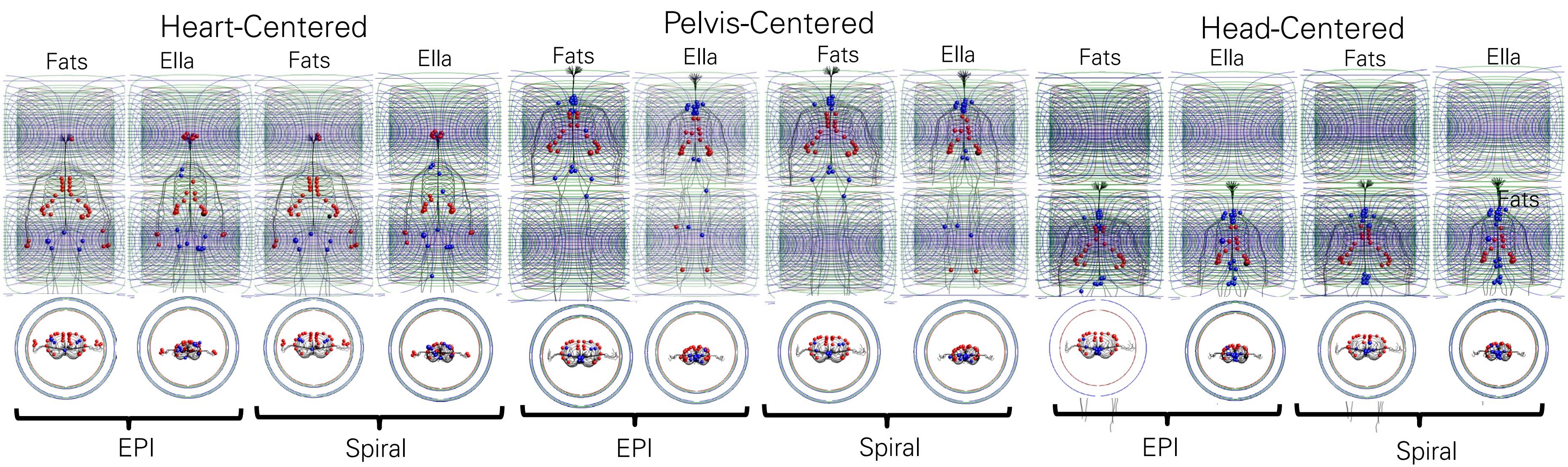

Values in [T/m/sec]		Fats		Ella	
	Sequence	End-Node	Not End-Node	End-Node	Not-End-Node
Head Centered	3D Spiral	196	258	259	387
	3D EPI	84	98	98	181
Heart Centered	3D Spiral	210	251	254	792
	3D EPI	84	89	117	260
Pelvis Centered	3D Spiral	169	356	208	489
	3D EPI	70	153	98	248

Slew rate (T/m/s) = rate of gradient field change → determines induced E-field magnitude

not end-node   end-node

MRI Gradient Safety: IEC 60601-2-33

- MRI gradient coils produce time-varying B-fields ($\frac{dB}{dt}$) → induce E-fields in the body → potential PNS [12]
- **Hyperbolic strength-duration model:**
  $\left.\frac{dB}{dt}\right|_{th} = I_{rh} \times \left(1 + \frac{\tau_{ch}}{t_{eff}}\right)$,
  default rheobase: $I_{rh} = 20\ \mathrm{T/s}$ [12]
- **Three operating modes:**
  - **Normal mode:** ≤80% of predicted PNS threshold — safe for all patients without supervision
  - **First-level controlled:** up to 100% of PNS threshold — may cause discomfort; requires medical supervision
  - **Second-level controlled:** exceeds first-level — requires special ethical/research approval

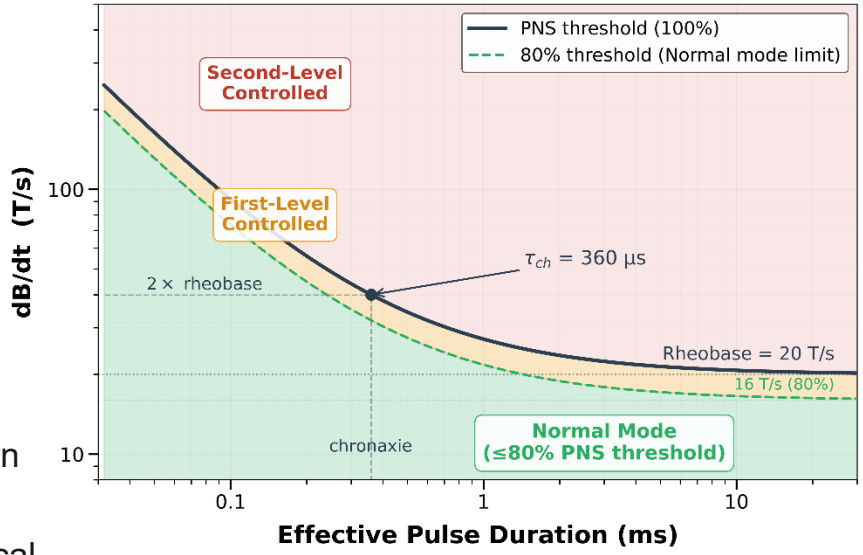

- **SAR limits by mode:** whole-body 2 / 4 / >4 W/kg; head 3.2 W/kg; local (10 g) 10 W/kg [12]
- Sim4Life ViP models used for gradient coil design validation and PNS threshold prediction [58]

Tissue Properties: Foundation of Accurate Modeling

- **IT'IS Tissue Properties Database** (itis.swiss/database): physical properties for 100+ tissue types [16]
  - Dielectric (RF and LF), thermal conductivity, density, perfusion, MRI relaxation times
- Built upon the foundational **Gabriel three-part measurement series** (1996): 10 Hz to 20 GHz [46, 47, 48]
  - Part III: four-term Cole-Cole dispersion model covering full frequency range
- **Critical for SCS:** CSF (~1.8 S/m), WM anisotropy, epidural fat, bone — all influence E-field distributions reaching dorsal roots [16]
- **LF challenges:**
  - Electrode polarization artifacts below ~1 MHz confound measurements
  - Substantial uncertainty in low-frequency conductivity values
  - Poorly characterized anisotropy in white matter and skeletal muscle
- **Same database** serves both therapeutic SCS simulation and safety assessment — shared-physics principle

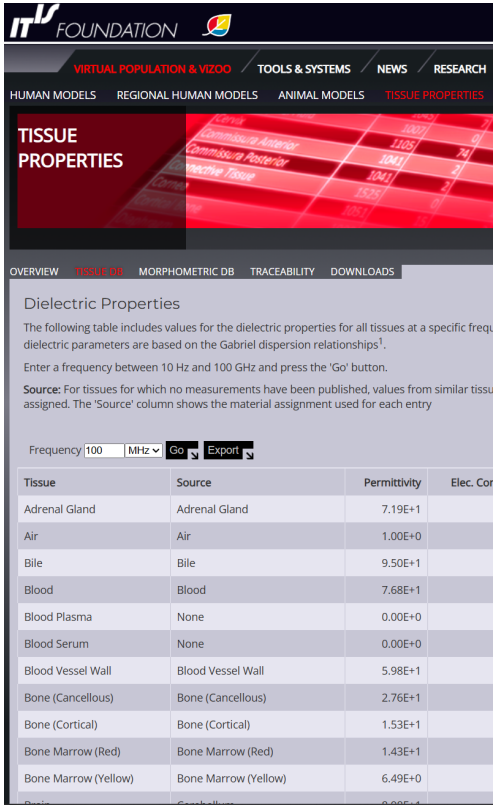

Image: [23]

Simulations in Research & Design

1. **Mechanism Investigation**
   - Coupled EM-neuro simulations reveal *which* neural elements are recruited and *why*
   - Capogrosso 2013 [3]: confirmed dorsal root recruitment; Formento 2018 [4]: predicted transient deafferentation
2. **Device Design**
   - In silico optimization of electrode geometry and waveform parameters
   - Holsheimer: narrow bipole/tripole [8], [33]; STIMO-2: 16-electrode paddle via Sim4Life [6]
3. **Personalization**
   - Patient-specific MRI segmentation → EM field prediction → optimized stimulation programs
   - 2 mm displacement → measurable selectivity loss [6]; reduces programming from weeks to minutes [5]
4. **Safety & Regulatory—same platform, opposite objective:** prevent unintended neural activation
   - LF exposure: ICNIRP/IEEE basic restrictions via ViP-based computational dosimetry [10], [11]
   - MRI gradient PNS: predict thresholds across body positions → IEC 60601-2-33 modes [12], [58]
   - MRI RF heating: SAR → Pennes bioheat → CEM43 thermal dose in ViP models [59], [60]
   - Implant safety (ISO/TS 10974): IT'IS IMAnalytics + MRIxViP = first computational FDA MDDT [13], [62]
   - *In silico* trials across Virtual Population reduce need for cadaver/animal studies

Images: Paddles and Personalized Model [18]; Spinal Field Distribution [8]

Simulations in Research & Design

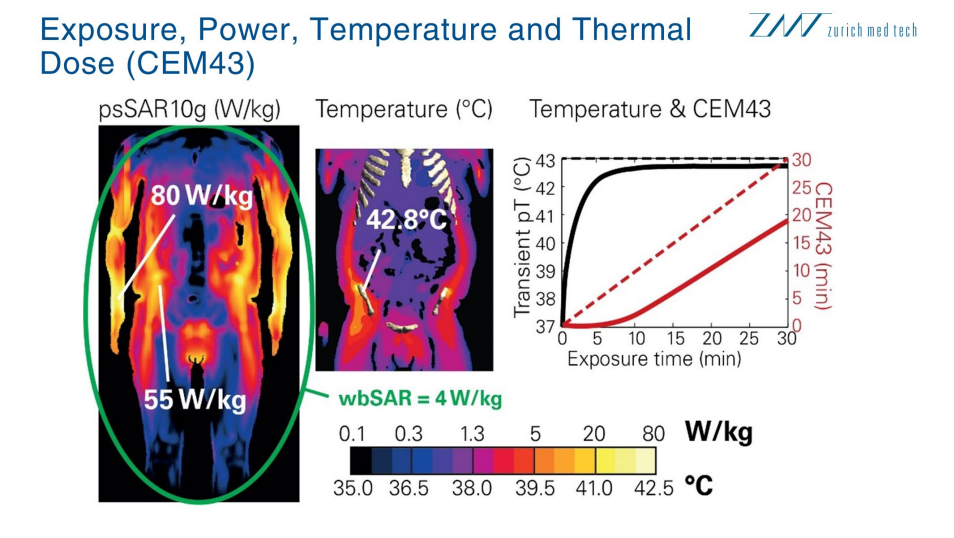

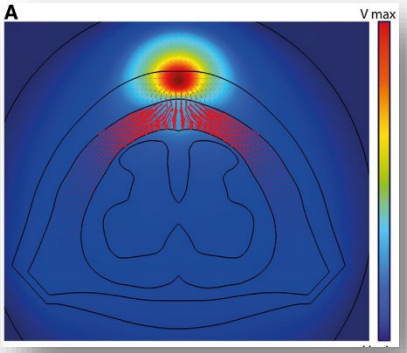

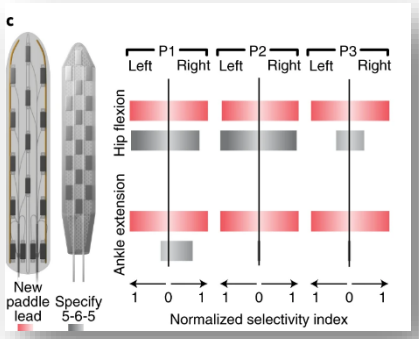

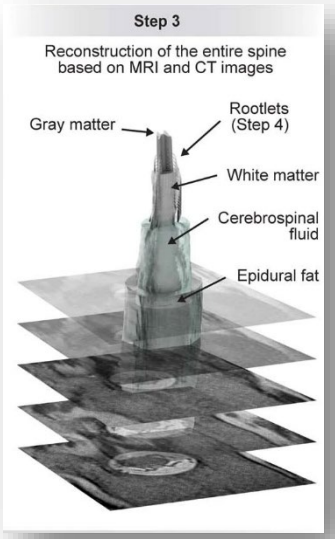

Images: Paddles and Personalized Model [18]; Spinal Field Distribution [8]

Key Takeaways

1. SCS evolved from gate control theory (1965) [1] through Shealy (1967) [2] to four pain paradigms and now locomotor restoration
2. The critical computational insight: **dorsal roots, not dorsal columns** are the target for locomotion [3] — geometry and the activating function (W3) explain why
3. Patient-specific models (IT'IS / Sim4Life) enabled the STIMO breakthrough: walking within one week [5]; complete paralysis reversed within one day [6]
4. The personalized pipeline is essential because anatomical variability (especially CSF thickness) makes standard approaches insufficient [8]
5. The pipeline applies coupled EM-neuro workflows (W4) to patient-specific spinal anatomy; optimization theory is covered in W11
6. LF exposure safety and MRI safety rest on the **same cable-equation biophysics** as therapeutic SCS [7], [10]
7. ICNIRP 2010 basic restrictions [10] and IEC 60601-2-33 operating modes [12] derive directly from PNS thresholds computed in ViP models
8. ISO/TS 10974 four-tier approach [13] + FDA-qualified IMAnalytics/MRIxViP [62] enable safe MRI scanning of SCS patients

Image Credits

1. Kim M, Jeong W, Jang S, Park JH, Bae Y, Lee SW. Spinal Cord Injury Epidemiology and Causes: A Worldwide Analysis with 2050 Projections. Healthcare (Basel). 2025 Oct 10;13(20):2552. doi: 10.3390/healthcare13202552. PMID: 41154231; PMCID: PMC12562789.
2. Fawcett, J., Curt, A., Steeves, J. et al. Guidelines for the conduct of clinical trials for spinal cord injury as developed by the ICCP panel: spontaneous recovery after spinal cord injury and statistical power needed for therapeutic clinical trials. Spinal Cord 45, 190–205 (2007). https://doi.org/10.1038/sj.sc.3102007
3. Google Gemini NanoBanana: Melzack & Wall, 1965. Theory of gate control for pain.
4. Mconnell, CC BY 3.0 <https://creativecommons.org/licenses/by/3.0>, via Wikimedia Commons
5. Google Gemini NanoBanana: Melzack & Wall, 1965. Stimulation waveforms for pain SCS.
6. Google Gemini NanoBanana: Melzack & Wall, 1965. Closed-loop SCS for pain using ECAPs.
7. CNX OpenStax, CC BY 4.0 <https://creativecommons.org/licenses/by/4.0>, via Wikimedia Commons
8. Capogrosso, et al., Journal of Neuroscience 4 December 2013, 33 (49) 19326-19340; https://doi.org/10.1523/JNEUROSCI.1688-13.2013
9. Luz, A., Rupp, R., Ahmadi, R. et al. Beyond treatment of chronic pain: a scoping review about epidural electrical spinal cord stimulation to restore sensorimotor and autonomic function after spinal cord injury. Neurol. Res. Pract. 5, 14 (2023). https://doi.org/10.1186/s42466-023-00241-z
10. Google Gemini NanoBanana: Melzack & Wall, 1965. Factors influencing dorsal root recruitment during EES.
11. Google Gemini NanoBanana. Current shunting in spine as a function of dorsal CSF thickness.
12. Rattay F, Minassian K, Dimitrijevic MR. Epidural electrical stimulation of posterior structures of the human lumbosacral cord: 2. quantitative analysis by computer modeling. Spinal Cord. 2000 Aug;38(8):473-89. doi: 10.1038/sj.sc.3101039. PMID: 10962608.
13. Struijk JJ, Holsheimer J, Boom HB. Excitation of dorsal root fibers in spinal cord stimulation: a theoretical study. IEEE Trans Biomed Eng. 1993 Jul;40(7):632-9. doi: 10.1109/10.237693. PMID: 8244424.
14. Wagner, F.B., Mignardot, JB., Le Goff-Mignardot, C.G. et al. Targeted neurotechnology restores walking in humans with spinal cord injury. Nature 563, 65–71 (2018). https://doi.org/10.1038/s41586-018-0649-2
15. Rowald, A., Komi, S., Demesmaeker, R. et al. Activity-dependent spinal cord neuromodulation rapidly restores trunk and leg motor functions after complete paralysis. Nat Med 28, 260–271 (2022). https://doi.org/10.1038/s41591-021-01663-5
16. Kathe, C., Skinnider, M.A., Hutson, T.H. et al. The neurons that restore walking after paralysis. Nature 611, 540–547 (2022). https://doi.org/10.1038/s41586-022-05385-7
17. https://ggba.swiss/en/onward-medical-receives-fda-authorization-for-its-spinal-cord-stimulation-system/
18. Rowald, A., Komi, S., Demesmaeker, R. et al. Activity-dependent spinal cord neuromodulation rapidly restores trunk and leg motor functions after complete paralysis. Nat Med 28, 260–271 (2022). https://doi.org/10.1038/s41591-021-01663-5
19. Sheldon BL, Bao J, Khazen O and Pilitsis JG (2021) Spinal Cord Stimulation as Treatment for Cancer and Chemotherapy-Induced Pain. Front. Pain Res. 2:699993. doi: 10.3389/fpain.2021.699993
20. https://www.bostonscientific.com/en-US/products/spinal-cord-stimulator-systems/scs_lead_portfolio.html
21. Google Gemini NanoBanana. Therapeutic vs. unintended nerve stimulation.
22. ICNIRP, "Guidelines for limiting exposure to time-varying electric and magnetic fields (1 Hz – 100 kHz)," *Health Physics*, vol. 99, no. 6, pp. 818–836, 2010.
23. https://itis.swiss/virtual-population/tissue-properties/database/dielectric-properties/

References

[1] R. Melzack and P. D. Wall, "Pain mechanisms: A new theory," *Science*, vol. 150, no. 3699, pp. 971–979, Nov. 1965. doi: 10.1126/science.150.3699.971.
[2] C. N. Shealy, J. T. Mortimer, and J. B. Reswick, "Electrical inhibition of pain by stimulation of the dorsal columns: Preliminary clinical report," *Anesth. Analg.*, vol. 46, no. 4, pp. 489–491, Jul.–Aug. 1967.
[3] M. Capogrosso, N. Wenger, S. Raspopovic, *et al.*, "A computational model for epidural electrical stimulation of spinal sensorimotor circuits," *J. Neurosci.*, vol. 33, no. 49, pp. 19326–19340, Dec. 2013. doi: 10.1523/JNEUROSCI.1688-13.2013.
[4] E. Formento, K. Minassian, F. Wagner, *et al.*, "Electrical spinal cord stimulation must preserve proprioception to enable locomotion in humans with spinal cord injury," *Nat. Neurosci.*, vol. 21, no. 12, pp. 1728–1741, Dec. 2018. doi: 10.1038/s41593-018-0262-6.
[5] F. B. Wagner, J.-B. Mignardot, C. G. Le Goff-Mignardot, *et al.*, "Targeted neurotechnology restores walking in humans with spinal cord injury," *Nature*, vol. 563, no. 7729, pp. 65–71, Nov. 2018. doi: 10.1038/s41586-018-0649-2.
[6] A. Rowald, S. Komi, R. Demesmaeker, *et al.*, "Activity-dependent spinal cord neuromodulation rapidly restores trunk and leg motor functions after complete paralysis," *Nat. Med.*, vol. 28, no. 2, pp. 260–271, Feb. 2022. doi: 10.1038/s41591-021-01663-5.
[7] F. Rattay, "Analysis of models for external stimulation of axons," *IEEE Trans. Biomed. Eng.*, vol. BME-33, no. 10, pp. 974–977, Oct. 1986. doi: 10.1109/TBME.1986.325670.
[8] J. Holsheimer, "Computer modelling of spinal cord stimulation and its contribution to therapeutic efficacy," *Spinal Cord*, vol. 36, no. 8, pp. 531–540, Aug. 1998. doi: 10.1038/sj.sc.3100717.
[9] J. Holsheimer, "Analysis of spinal cord stimulation and design of epidural electrodes by computer modeling," *Neuromodulation*, vol. 1, no. 1, pp. 14–18, 1998. doi: 10.1111/j.1525-1403.1998.tb00026.x.
[10] ICNIRP, "Guidelines for limiting exposure to time-varying electric and magnetic fields (1 Hz to 100 kHz)," *Health Phys.*, vol. 99, no. 6, pp. 818–836, Dec. 2010. doi: 10.1097/HP.0b013e3181f06c86.
[11] IEEE Std C95.1-2019, "IEEE Standard for safety levels with respect to human exposure to electric, magnetic, and electromagnetic fields, 0 Hz to 300 GHz," Oct. 2019.
[12] IEC 60601-2-33:2022, "Medical electrical equipment — Part 2-33: Particular requirements for the basic safety and essential performance of magnetic resonance equipment for medical diagnosis," 4th ed.
[13] ISO/TS 10974:2018, "Assessment of the safety of magnetic resonance imaging for patients with an active implantable medical device," 2nd ed.
[14] C. C. McIntyre, A. G. Richardson, and W. M. Grill, "Modeling the excitability of mammalian nerve fibers: Influence of afterpotentials on the recovery cycle," *J. Neurophysiol.*, vol. 87, no. 2, pp. 995–1006, Feb. 2002. doi: 10.1152/jn.00353.2001.
[15] L. Kapural, C. Yu, M. W. Doust, *et al.*, "Novel 10-kHz high-frequency therapy (HF10 therapy) is superior to traditional low-frequency spinal cord stimulation for the treatment of chronic back and leg pain: The SENZA-RCT randomized controlled trial," *Anesthesiology*, vol. 123, no. 4, pp. 851–860, Oct. 2015. doi: 10.1097/ALN.0000000000000774.
[16] IT'IS Foundation, "Database of tissue properties," [Online]. Available: https://itis.swiss/virtual-population/tissue-properties/database/
[17] A. Kumar *et al.*, "Global incidence, prevalence, and years lived with disability of spinal cord injury, 1990–2019," *Lancet Neurol.*, vol. 22, no. 11, pp. 1026–1047, 2023. doi: 10.1016/S1474-4422(23)00336-4.
[18] R. Melzack, "Gate control theory: On the evolution of pain concepts," *Pain Forum*, vol. 5, no. 2, pp. 128–138, 1996. doi: 10.1016/S1082-3174(96)80050-X.
[19] C. N. Shealy, J. T. Mortimer, and N. R. Hagfors, "Dorsal column electroanalgesia," *J. Neurosurg.*, vol. 32, no. 5, pp. 560–564, May 1970. doi: 10.3171/jns.1970.32.5.0560.
[20] B. Linderoth and R. D. Foreman, "Physiology of spinal cord stimulation: Review and update," *Neuromodulation*, vol. 2, no. 3, pp. 150–164, 1999. doi: 10.1046/j.1525-1403.1999.00150.x.
[21] D. De Ridder, S. Vanneste, M. Plazier, E. van der Loo, and T. Menovsky, "Burst spinal cord stimulation: Toward paresthesia-free pain suppression," *Neurosurgery*, vol. 66, no. 5, pp. 986–990, May 2010. doi: 10.1227/01.NEU.0000368153.44883.B3.
[22] T. Deer, K. V. Slavin, K. Amirdelfan, *et al.*, "Success Using Neuromodulation with BURST (SUNBURST) study: Results from a prospective, randomized controlled trial using a novel burst waveform," *Neuromodulation*, vol. 21, no. 1, pp. 56–66, Jan. 2018. doi: 10.1111/ner.12698.
[23] Nevro Corp., "Nevro receives FDA approval for Senza spinal cord stimulation system," Press Release, May 8, 2015. (PMA P130022.)
[24] L. Kapural, C. Yu, M. W. Doust, *et al.*, "Comparison of 10-kHz high-frequency and traditional low-frequency spinal cord stimulation for the treatment of chronic back and leg pain: 24-month results," *Neurosurgery*, vol. 79, no. 5, pp. 667–677, Nov. 2016. doi: 10.1227/NEU.0000000000001418.
[25] T. R. Deer, R. M. Levy, J. Kramer, *et al.*, "Dorsal root ganglion stimulation yielded higher treatment success rate for complex regional pain syndrome and causalgia at 3 and 12 months: A randomized comparative trial," *Pain*, vol. 158, no. 4, pp. 669–681, Apr. 2017. doi: 10.1097/j.pain.0000000000000814.
[26] N. Mekhail, R. M. Levy, T. R. Deer, *et al.*, "Long-term safety and efficacy of closed-loop spinal cord stimulation to treat chronic back and leg pain (Evoke): A double-blind, randomised, controlled trial," *Lancet Neurol.*, vol. 19, no. 2, pp. 123–134, Feb. 2020. doi: 10.1016/S1474-4422(19)30414-4.
[27] N. A. Mekhail, R. M. Levy, T. R. Deer, *et al.*, "ECAP-controlled closed-loop versus open-loop SCS for the treatment of chronic pain: 36-month results of the EVOKE blinded randomized clinical trial," *Reg. Anesth. Pain Med.*, vol. 49, no. 5, pp. 346–354, May 2024. doi: 10.1136/rapm-2023-104751.
[28] Medtronic, "FDA approves Medtronic Inceptiv closed-loop spinal cord stimulator," Press Release, 2024.
[29] J. J. Struijk, J. Holsheimer, B. K. van Veen, and H. B. K. Boom, "Epidural spinal cord stimulation: Calculation of field potentials with special reference to dorsal column nerve fibers," *IEEE Trans. Biomed. Eng.*, vol. 38, no. 1, pp. 104–110, Jan. 1991. doi: 10.1109/10.68217.

References

[30] J. J. Struijk, J. Holsheimer, and H. B. K. Boom, "Excitation of dorsal root fibers in spinal cord stimulation: A theoretical study," *IEEE Trans. Biomed. Eng.*, vol. 40, no. 7, pp. 632–639, Jul. 1993. doi: 10.1109/10.237693.
[31] D. R. McNeal, "Analysis of a model for excitation of myelinated nerve," *IEEE Trans. Biomed. Eng.*, vol. 23, no. 4, pp. 329–337, Jul. 1976. doi: 10.1109/TBME.1976.324593.
[32] J. J. Struijk, J. Holsheimer, G. G. van der Heide, and H. B. K. Boom, "Recruitment of dorsal column fibers in spinal cord stimulation: Influence of collateral branching," *IEEE Trans. Biomed. Eng.*, vol. 39, no. 9, pp. 903–912, Sep. 1992. doi: 10.1109/10.256423.
[33] J. Holsheimer and W. A. Wesselink, "Optimum electrode geometry for spinal cord stimulation: The narrow bipole and tripole," *Med. Biol. Eng. Comput.*, vol. 35, pp. 493–497, 1997. doi: 10.1007/BF02525529.
[34] F. Rattay, K. Minassian, and M. R. Dimitrijevic, "Epidural electrical stimulation of posterior structures of the human lumbosacral cord: 2. Quantitative analysis by computer modeling," *Spinal Cord*, vol. 38, pp. 473–489, 2000. doi: 10.1038/sj.sc.3101039.
[35] F. Rattay, "The basic mechanism for the electrical stimulation of the nervous system," *Neuroscience*, vol. 89, no. 2, pp. 335–346, Mar. 1999. doi: 10.1016/S0306-4522(98)00330-3.
[36] N. Wenger, E. M. Moraud, *et al.*, "Spatiotemporal neuromodulation therapies engaging muscle synergies improve motor control after spinal cord injury," *Nat. Med.*, vol. 22, no. 2, pp. 138–145, Feb. 2016. doi: 10.1038/nm.4025.
[37] M. Capogrosso, *et al.*, "Configuration of electrical spinal cord stimulation through real-time processing of gait kinematics," *Nat. Protoc.*, vol. 13, no. 9, pp. 2031–2061, Sep. 2018. doi: 10.1038/s41596-018-0030-9.
[38] C. Kathe, M. A. Skinnider, T. H. Hutson, *et al.*, "The neurons that restore walking after paralysis," *Nature*, vol. 611, no. 7936, pp. 540–547, Nov. 2022. doi: 10.1038/s41586-022-05385-7.
[39] H. Lorach, A. Galvez, V. Spagnolo, *et al.*, "Walking naturally after spinal cord injury using a brain–spine interface," *Nature*, vol. 618, no. 7963, pp. 126–133, Jun. 2023. doi: 10.1038/s41586-023-06094-5.
[40] T. Milekovic, E. M. Moraud, N. Macellari, *et al.*, "A spinal cord neuroprosthesis for locomotor deficits due to Parkinson's disease," *Nat. Med.*, vol. 29, pp. 2854–2865, 2023. doi: 10.1038/s41591-023-02584-1.
[41] N. Cho, J. W. Squair, V. Aureli, *et al.*, "Hypothalamic deep brain stimulation augments walking after spinal cord injury," *Nat. Med.*, vol. 30, no. 12, pp. 3676–3686, Dec. 2024. doi: 10.1038/s41591-024-03306-x.
[42] A. A. Phillips, A. P. Gandhi, N. Hankov, *et al.*, "An implantable system to restore hemodynamic stability after spinal cord injury," *Nat. Med.*, 2025. doi: 10.1038/s41591-025-03614-w.
[43] ONWARD Medical NV, corporate history and regulatory milestones per SEC/Euronext filings and press releases, 2014–2026.
[44] C. Moritz, E. Field-Fote, *et al.*, "Non-invasive spinal cord electrical stimulation for arm and hand function in chronic tetraplegia: A safety and efficacy trial," *Nat. Med.*, vol. 30, pp. 1276–1283, 2024. doi: 10.1038/s41591-024-02940-9.
[45] E. Neufeld, D. Szczerba, N. Chavannes, and N. Kuster, "A novel medical image data-based multi-physics simulation platform for computational life sciences," *Interface Focus*, vol. 3, no. 2, p. 20120058, Apr. 2013. doi: 10.1098/rsfs.2012.0058.
[46] C. Gabriel, S. Gabriel, and E. Corthout, "The dielectric properties of biological tissues: I. Literature survey," *Phys. Med. Biol.*, vol. 41, no. 11, pp. 2231–2249, Nov. 1996. doi: 10.1088/0031-9155/41/11/001.
[47] S. Gabriel, R. W. Lau, and C. Gabriel, "The dielectric properties of biological tissues: II. Measurements in the frequency range 10 Hz to 20 GHz," *Phys. Med. Biol.*, vol. 41, no. 11, pp. 2251–2269, Nov. 1996. doi: 10.1088/0031-9155/41/11/002.
[48] S. Gabriel, R. W. Lau, and C. Gabriel, "The dielectric properties of biological tissues: III. Parametric models for the dielectric spectrum of tissues," *Phys. Med. Biol.*, vol. 41, no. 11, pp. 2271–2293, Nov. 1996. doi: 10.1088/0031-9155/41/11/003.
[49] R. B. North, D. H. Kidd, L. Petrucci, and M. J. Dorsi, "Spinal cord stimulation electrode design: A prospective, randomized, controlled trial comparing percutaneous with laminectomy electrodes: Part II–Clinical outcomes," *Neurosurgery*, vol. 57, no. 5, pp. 990–996, Nov. 2005. doi: 10.1227/01.NEU.0000180030.00167.b9.
[50] T. H. Newton, J. G. Ordonez, E. Neufeld, and N. Kuster, "Optimizing spinal cord stimulation using a novel Green's function-based generalized activating function," *Neuromodulation*, vol. 26, Suppl. 1, p. S44, 2023 (NANS 2023 abstract). doi: 10.1016/j.neurom.2023.01.028.
[51] E. Mirzakhalili, E. R. Rogers, and S. F. Lempka, "An optimization framework for targeted spinal cord stimulation," *J. Neural Eng.*, vol. 20, no. 5, p. 056026, Sep. 2023. doi: 10.1088/1741-2552/acf522.
[52] o2S2PARC, "Open Online Simulations for Stimulating Peripheral Activity to Relieve Conditions," [Online]. Available: https://osparc.io
[53] G. Weiss, "Sur la possibilité de rendre comparables entre eux les appareils servant à l'excitation électrique," *Arch. Ital. Biol.*, vol. 35, pp. 413–446, 1901.
[54] L. Lapicque, "Définition expérimentale de l'excitabilité," *C. R. Séances Soc. Biol. Fil.*, vol. 67, pp. 280–283, 1909. **[CORRECTED: was incorrectly listed as *C. R. Acad. Sci.*]**
[55] D. Boinagrov, J. Loudin, and D. Palanker, "Strength–duration relationship for extracellular neural stimulation: Numerical and analytical models," *J. Neurophysiol.*, vol. 104, pp. 2236–2248, 2010. doi: 10.1152/jn.00343.2010.
[56] A. Christ, W. Kainz, E. G. Hahn, *et al.*, "The Virtual Family — Development of surface-based anatomical models of two adults and two children for dosimetric simulations," *Phys. Med. Biol.*, vol. 55, no. 2, pp. N23–N38, Jan. 2010. doi: 10.1088/0031-9155/55/2/N01.

References

[57] M.-C. Gosselin, E. Neufeld, H. Moser, *et al.*, "Development of a new generation of high-resolution anatomical models for medical device evaluation: The Virtual Population 3.0," *Phys. Med. Biol.*, vol. 59, no. 18, pp. 5287–5303, Sep. 2014. doi: 10.1088/0031-9155/59/18/5287.
[58] M. Davids, B. Guérin, A. vom Endt, L. R. Schad, and L. L. Wald, "Prediction of peripheral nerve stimulation thresholds of MRI gradient coils using coupled electromagnetic and neurodynamic simulations," *Magn. Reson. Med.*, vol. 81, no. 1, pp. 686–701, 2019. doi: 10.1002/mrm.27382.
[59] G. C. van Rhoon, T. Samaras, P. S. Yarmolenko, M. W. Dewhirst, E. Neufeld, and N. Kuster, "CEM43°C thermal dose thresholds: A potential guide for magnetic resonance radiofrequency exposure levels?," *Eur. Radiol.*, vol. 23, no. 8, pp. 2215–2227, 2013. doi: 10.1007/s00330-013-2825-y.
[60] H. H. Pennes, "Analysis of tissue and arterial blood temperatures in the resting human forearm," *J. Appl. Physiol.*, vol. 1, no. 2, pp. 93–122, 1948. doi: 10.1152/jappl.1948.1.2.93.
[61] S.-M. Park, R. Kamondetdacha, and J. A. Nyenhuis, "Calculation of MRI-induced heating of an implanted medical lead wire with an electric field transfer function," *J. Magn. Reson. Imaging*, vol. 26, no. 5, pp. 1278–1285, Nov. 2007. doi: 10.1002/jmri.21159.
[62] IT'IS Foundation, "IMAnalytics and MRIxViP receive FDA Medical Device Development Tool qualification," Dec. 2019. [Online]. Available: https://itis.swiss/news-events/news/
[63] Holsheimer J, den Boer JA, Struijk JJ, Rozeboom AR. MR assessment of the normal position of the spinal cord in the spinal canal. AJNR Am J Neuroradiol. 1994 May;15(5):951-9. PMID: 8059666; PMCID: PMC8332172.